INL/MIS-24-79988-Revision-0

Path Toward a Breeding, Proliferation-Resistant, Thermal-Spectrum Molten Salt Reactor

February 2025

David Eugene Holcomb, Mauricio Eduardo Tano Retamales

Changing the World's Energy Future

Idaho National Laboratory

INL is a U.S. Department of Energy National Laboratory operated by Battelle Energy Alliance, LLC

INL/MIS-24-79988-Revision-0

Path Toward a Breeding, Proliferation-Resistant, Thermal-Spectrum Molten Salt Reactor

David Eugene Holcomb, Mauricio Eduardo Tano Retamales

February 2025

Idaho National Laboratory
Idaho Falls, Idaho 83415

http://www.inl.gov

Prepared for the
U.S. Department of Energy
Under DOE Idaho Operations Office
Contract DE-AC07-05ID14517

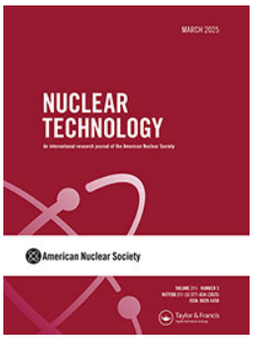

Nuclear Technology

ISSN: (Print) (Online) Journal homepage: www.tandfonline.com/journals/unct20

Path Toward a Breeding, Proliferation-Resistant, Thermal-Spectrum Molten Salt Reactor

David E. Holcomb & Mauricio E. Tano

To cite this article: David E. Holcomb & Mauricio E. Tano (12 Feb 2025): Path Toward a Breeding, Proliferation-Resistant, Thermal-Spectrum Molten Salt Reactor, Nuclear Technology, DOI: 10.1080/00295450.2024.2431776

To link to this article: https://doi.org/10.1080/00295450.2024.2431776

Published online: 12 Feb 2025.

NUCLEAR TECHNOLOGY

DOI: https://doi.org/10.1080/00295450.2024.2431776

Path Toward a Breeding, Proliferation-Resistant, Thermal-Spectrum Molten Salt Reactor

David E. Holcomb* and Mauricio E. Tano

Idaho National Laboratory, Advanced Reactor Technology, 1955 Fremont Avenue, Idaho Falls, Idaho 83415

Received August 29, 2024
Accepted for Publication November 15, 2024

Abstract — *Liquid-fueled, thermal-spectrum molten salt breeder reactors (TS-MSBRs) offer the potential for affordable, safe, inexhaustible energy with minimal potential for nuclear material misuse and without significant actinide waste generation. Realizing the full set of TS-MSBR capabilities is only now becoming possible with the advent of advanced fuel-salt processing techniques, improved materials, and a more detailed understanding of fuel-salt properties. Additionally, modern higher-fidelity modeling and simulation methods enable a more detailed evaluation of TS-MSBR design options. TS-MSBRs, however, remain immature and will require substantial, sustained development resources.*

Keywords — *Molten salt breeder reactor, proliferation resistant, thermal spectrum, fuel cycle.*

Note — *Some figures may be in color only in the electronic version.*

I. INTRODUCTION

The original goal of the historic thermal-spectrum molten-salt breeder reactor (TS-MSBR) program remains laudable: to develop molten-salt reactors as commercial nuclear power plants (NPPs) with low fissile inventory and breeding gain to limit the demand on natural fissile resources. The historic TS-MSBR program envisioned employing the thorium-uranium (Th-U) fuel cycle. However, the program did not focus on minimizing the potential to misuse fissile materials for nonpeaceful purposes.[1] Over the half-century since the cancellation of the historic TS-MSBR program, fuel-salt processing concepts and technologies have advanced substantially outside of the United States. A proliferation-resistant, thermal-spectrum, liquid-fuel molten salt reactor (MSR) fuel cycle with net breeding gain now appears possible via a combination of advanced fuel-salt processing technologies and improved materials, along with an optimized core configuration.

This paper is organized as a roadmap for a novel TS-MSBR concept. This roadmap begins with a discussion of why liquid-fueled reactors have such great potential. The first section provides the reasons behind the shutdown of the historic TS-MSBR program and describes how technological progress could enable the development of a proliferation-resistant TS-MSBR with attractive performance characteristics. The roadmap then continues with an overview of a conceptual design for a novel TS-MSBR that leverages recent progress in salt processing technologies and salt-compatible structural materials.

Next, the roadmap describes how the concerns raised by the historic, independent, expert reviews of

*E-mail: David.Holcomb@inl.gov

TS-MSBRs can be, or have already been, addressed. The roadmap then discusses the public and private partnership necessary to commercialize MSRs that meet both private sector requirements and U.S. government objectives. Finally, the roadmap provides an overview of why the costs for MSBRs have the potential to be substantially lower than those of recent NPPs.

II. BACKGROUND AND RATIONALE

The major distinguishing aspect of MSRs is the liquid state of their fuel. Liquid-fueled reactors were among the earliest reactor classes proposed, having origins in the Manhattan Project.[2,3] By the late 1940s, work had started on high-temperature fluid fuel. Much of the initial development work was sponsored by the U.S. Air Force, resulting in the first MSR (the Aircraft Reactor Experiment) in 1954.[4] The 1959 "Report of the Fluid Fuel Reactors Task Force"[5] concentrated fluid-fuel development efforts on reactors employing high-temperature, liquid-halide salts as fuel.

Nuclear fuel serves two main purposes: generating power through fission and dissipating the resulting heat to a coolant. Liquid fuel offers advantages for both functions. In terms of power generation, its liquid state significantly simplifies the process of adding or removing fissile and fertile material, as well as the online removal of parasitic neutron absorbers. Maintaining only the necessary amount of fuel in the core enhances fissile material utilization efficiency, avoiding the need for neutron poisons, and reduces the risk of reactivity-based accidents. The liquid state also facilitates the removal of fuel from the critical region as a safety response. In contrast, solid reactor fuels, like those in CANDU (Canada deuterium uranium) and pebble bed reactors, can approximate continuous fuel addition and removal but struggle with the practical removal of parasitic neutron absorbers such as ^{135}Xe.

Liquid salts excel in high-temperature heat transfer, contributing to high plant thermodynamic efficiency. Solid fuels rely on conduction for fission power transfer, while liquid fuels leverage both conduction and convection for heat transfer. Additionally, liquid salt boasts the highest exergy among reactor classes due to its high boiling temperature and effective heat transfer. This high exergy is particularly important for supporting thermochemical processes like hydrogen production,[6] subsequently facilitating the production of liquid hydrocarbon biofuels.[7]

The lifespan of solid fuel is determined by a combination of radiation damage and decrease in reactivity, stemming from the (potentially uneven) depletion of fissile material and the buildup of parasitic absorbers. At the end of its useful life, solid fuel transforms into high-level waste. Even when spent fuel undergoes reprocessing, the resulting waste materials also qualify as high-level waste, necessitating long-term storage at an additional cost. In contrast, liquid fuel cannot be mechanically damaged, and its composition can be adjusted as part of normal operations. Liquid fuel, with effective removal of contaminants and parasitic absorbers, boasts an indefinite lifespan (potentially spanning multiple generations of reactors), allowing even thermal-spectrum systems to consume heavy actinides. An additional challenge is developing materials for reactor structures or replacement strategies that are compatible with the expected lifetime of the NPP.

II.A. Thermal-Spectrum Breeder Comparison to Other MSR Concepts

Nonbreeding, thermal-spectrum molten salt reactors (TS-MSRs) and fast-spectrum MSBRs also offer attractive features while maintaining the positive attributes common to MSRs. A comparative summary of MSRs by spectrum and fuel breeding function is provided in Table I. The attributes included in this table are expanded in the following paragraphs.

Thermal-spectrum molten salt reactors operating on the once-through uranium-plutonium (U-Pu) fuel cycle can be simpler than thermal breeders, thanks to reduced interconnected fuel-salt processing. However, thermal-spectrum burner MSRs face similar fuel cycle challenges as light water–cooled reactors (LWRs). Specifically, they rely on enriched uranium and generate actinide-bearing wastes. In the once-through U-Pu fuel cycle, uranium enrichment stands out as the most proliferation-vulnerable step. In the absence of substantial fuel-salt processing, used fuel salt will eventually transform into high-level waste due to the accumulation of parasitic neutron absorbers.

Just over 4% of the world's primary energy is generated by nuclear power (just over 10% of electricity).[8] Nuclear reactors have the potential to become a preferred primary energy source. While uranium reserves are substantial, breeding will eventually become necessary if nuclear power use is to expand to sustainably provide a significant portion of the world's primary energy.

Both fast-spectrum MSRs and TS-MSRs can be configured to support breeding. Fast-spectrum MSBRs enable efficient heavy metal resource utilization, effectively consume nonfissile actinides, and provide strongly negative temperature-reactivity feedback. However, fission cross

TABLE I

Comparative Summary of Thermal-Spectrum and Fast-Spectrum MSRs with Breeding and Nonbreeding Functions

Breeding/ Spectrum	Thermal	Fast
Nonbreeder	Salt processing needs: lower than breeder; volume: smaller; fuel supply needs: higher than breeder; high-level waste: higher; fuel-salt melting temperature: lower; uranium enrichment needed: LEU; irradiation damage: lower	Salt processing needs: lower than breeder; volume: larger; fuel supply needs: higher than breeder; high-level waste: higher (due to larger fuel-salt volume); fuel-salt melting temperature: higher; uranium enrichment needed: high-assay low-enrichment uranium; irradiation damage: higher
Breeder	Salt processing needs: higher than nonbreeder; volume: smaller; fuel supply needs: lower than nonbreeder; high-level waste: lower; fuel-salt melting temperature: lower; uranium enrichment needed: LEU; irradiation damage: lower	Salt processing needs: higher than nonbreeder; volume: larger; fuel supply needs: lower than nonbreeder; high-level waste: lower (due to indefinite fuel salt lifetime); fuel salt melting temperature: higher; uranium enrichment needed: high-assay low-enrichment uranium; irradiation damage: higher

sections are much lower in the fast-energy region, necessitating substantially larger (8- to 10-fold) amounts of fissile resources to achieve initial criticality. In addition, the melting temperature of fuel salts with sufficient fissile loading for a fast-spectrum MSR tends to be higher than that of thermal-spectrum fuel salts, necessitating more advanced container materials. Moreover, the low-fission cross sections result in the need for larger core sizes for efficient operation, inhibiting the development of smaller power plants. Additionally, fast-spectrum MSRs impart much higher fast-flux radiation damage to components near the critical region.

Thermal-spectrum reactors can be more rapidly scaled into widespread usage due to their lower initial fissile material requirements and less challenging material requirements, which result from their lower fuel-salt melting temperature and lower radiation damage. Thermal-spectrum reactors transition more rapidly (following initial startup) to highly unattractive isotopic compositions; they efficiently consume fissile isotopes while the nonfissile isotopes build up to equilibrium concentrations.[9]

II.B. Why MSRs Were Not Developed Previously and What Has Changed

A reasonable question for TS-MSBRs is: With such great potential recognized so long ago, why haven't TS-MSBRs already been developed? The three basic elements of the rationale for the lack of development are as follows:

1. *TS-MSBRs have not been necessary*. The development and deployment of new technology always incurs costs and risks. The U.S. electricity grid has been amply and economically supplied with electricity via fossil fuels and LWRs operating on the once-through U-Pu fuel cycle. The slow rate of demand growth over the past few decades has inhibited the introduction of any advanced reactor technology.

2. *TS-MSBR technology and related supply chain challenges have not yet been overcome*. MSRs have been judged as too risky and insufficiently important to justify the investment of the resources necessary to overcome their remaining technical hurdles. The United States historically pursued two breeder reactor options: the sodium-cooled fast reactor (SFR) and the TS-MSBR. The SFR was the lead option, and consequently, received the majority of the resources. Funding for the TS-MSBR program was stopped when the United States decided to pursue only a single breeder reactor concept.

3. *Proliferation resistance became prominent just as the historic program required expanded resources*. The need to minimize the potential to misuse fissile materials was not central to the historic TS-MSBR program. The historically proposed TS-MSBR fuel cycle included several steps with relatively direct access to unacceptably attractive nuclear material.

The MSR development and deployment rationale is significantly different today as follows:

1. The world has a large and growing need for affordable, dispatchable, clean energy production, including both electricity and high-exergy process heat. LWR costs have proven to be sufficiently high to significantly inhibit expanded deployment. While gas-cooled reactors

have higher core outlet temperatures, MSRs deliver their heat over a narrow high-temperature band, resulting in the highest exergy process heat of any reactor class, and are well suited to expand the application of nuclear power beyond electricity generation to thermochemical processes.

2. Technology has advanced substantially, and pathways have been identified to address all the identified TS-MSBR technology issues (see following sections). TS-MSBRs have the potential to provide a unique combination of advantageous reactor features, including fully passive safety, high fissile resource efficiency and low inventory, avoidance of significant actinide waste generation, high thermal efficiency, lower capital cost, lower fuel cycle cost, and strong proliferation resistance.

3. TS-MSBR integrated reactor and fuel cycles have been identified that avoid generating materials more attractive than low-enriched uranium (LEU) and avoid the need for future uranium enrichment following fuel cycle startup.

III. CONCEPTUAL DESIGN OF THE MSBR

This section introduces a conceptual design for a proliferation-resistant TS-MSBR. The section is organized as follows. First, it describes the technical basis of the fuel cycle and the proposed conceptual design for the MSBR. Then engineering results showing the optimization of the reactor core and the fuel cycle separations processes are provided. Finally, issues related to proliferation resistance and materials selection are addressed.

III.A. Fuel Cycle Overview

The proposed fuel cycle for a modern, proliferation-resistant, TS-MSBR blends the Th-U and U-Pu fuel cycles to obtain net breeding while maintaining low material attractiveness for the nuclear fuel. The neutron interaction processes with the fuel are shown schematically in Fig. 1. The equilibrium fuel-salt feedstock contains both natural (or depleted) uranium and thorium. In a breeding Th-U fuel cycle, neutrons are captured in fertile ^{232}Th, which then decays via beta minus to ^{233}Pa, and subsequently decays, again by beta minus, to fissile ^{233}U. Protactinium-233, however, has both a high parasitic neutron capture cross section (~20 b at 90 meV, i.e., for fully thermalized neutrons at MSR operating temperature) and a ~27-day half-life, which can result in parasitic neutron absorption into nonfissile ^{234}U. Figure 1 shows the capture sequence and typical thermal-spectrum branching ratios. The ^{233}Pa needs to be removed from a high neutron flux environment to decay for several half-lives to achieve net breeding gain.

While Th-U breeding gain has been demonstrated in solid oxide fuel under the light water breeder reactor development program,[10] and multiple different Th-U fuel cycle options were evaluated as part of the U.S. Department of Energy (DOE) Fuel Cycle Options program,[11] most of these prior evaluations have not focused on the capabilities enabled by liquid fuel. In particular, the liquid state facilitates quasi online access to the fuel.

The method proposed in the historic TS-MSBR program to enable ^{233}Pa to decay into ^{233}U in a very low-flux environment was to remove the ^{233}Pa from the core. Isolating the ^{233}Pa, however, results in the creation of material that is more attractive than LEU, as the ^{233}Pa

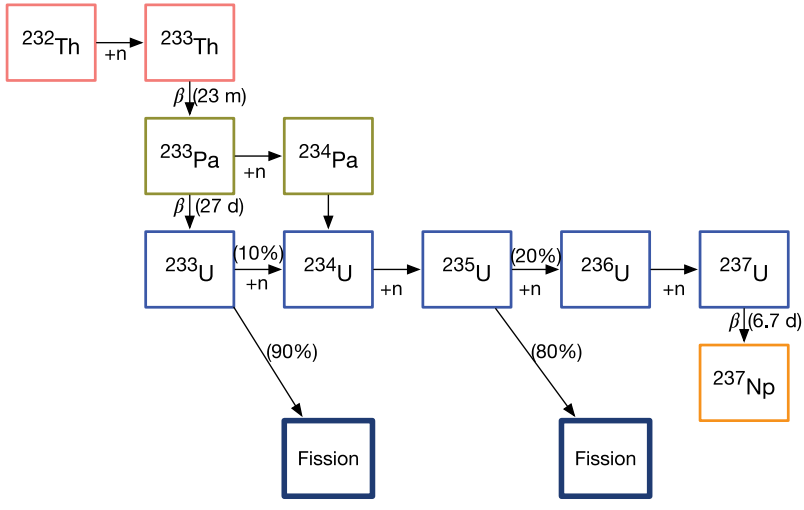

Fig. 1. Thorium-uranium neutron interactions with typical thermal-spectrum branching ratios.

decays to ^{233}U. Creation of unacceptably attractive material while maintaining a breeding gain was a primary issue that the historic TS-MSBR program never overcame.

To enable ^{232}Th breeding, the ratio of neutron absorption in ^{232}Th to absorption in ^{238}U needs to be maximized. The ^{232}Th absorption probability can be maximized both by increasing the concentration ratio of thorium to uranium in the fuel salt and by providing a low-energy neutron spectrum at the location of the fuel salt, i.e., by employing a heterogeneous core design with substantial moderation. Thorium-232 has a higher neutron absorption cross section than ^{238}U in the thermal neutron energy region. Figure 2 depicts the absorption cross section of these isotopes over the thermal energy range.

Thermal neutron absorption in ^{238}U would be somewhat parasitic due to the number of neutrons produced per neutron absorbed (reproduction factor or η) of bred-in ^{239}Pu being less than two for low-energy neutrons. Fluoride salts can incorporate substantial quantities of ThF_4 while maintaining an adequately low melting point. The key requirement establishing the minimum uranium (mixture of ^{233}U, ^{235}U, and ^{238}U) quantity is maintaining criticality. The startup fuel-salt loads need to have a somewhat higher uranium and lower thorium concentrations to compensate for the lower neutron yield per thermal fission of ^{235}U as compared to ^{233}U.

Breeding in a thermal-spectrum Th-U fuel cycle requires the efficient removal of parasitic neutron absorbers. Fission products have much larger neutron absorption cross sections for thermal neutrons. Multiple different processes are available to strip parasitic absorbers from barren (fuel free) salt, such as melt recrystallization, distillation, or oxidative precipitation. Gaseous, absorber precursor (e.g., ^{135}I), and insoluble (noble) fission products, contaminants, and corrosion products would also be removed from the barren salt.

III.B. Reactor Configuration Conceptual Overview

As described in the previous section, efficient moderation along with an optimized core configuration and minimal parasitic absorption are key to achieving breeding gain in the proposed fuel cycle. A heterogeneous core configuration, i.e., fuel salt in tubes surrounded by unfueled coolant salt and a high-temperature moderator, will be employed with a substantial moderator volume to enable fission neutrons to thermalize away from resonance absorption in the fuel. Employing an unfueled coolant also substantially reduces the neutron dose to the reactor vessel and the radiation levels within containment.

A conceptual core design for this initial proposed reactor concept is depicted in Fig. 3. The heterogeneous core consists of circular tubes of fuel salt that are surrounded by annular tubes for the coolant salt. A structural NbC-Be_2C casing (analogous to solid fuel cladding) separates the fuel and coolant salt, and a series of periodically spaced tubes are embedded into the moderator matrix. FLiBe (2^7LiF-BeF_2) is employed as coolant salt, as it has minimal activation, good material compatibility characteristics, strong heat transfer characteristics, and provides the best neutronic performance of any reasonable halide salt.

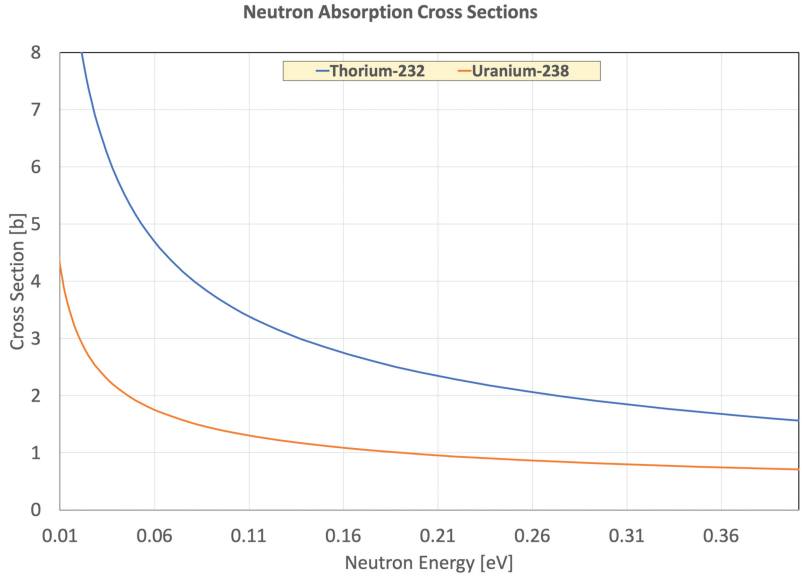

Fig. 2. Neutron absorption cross sections for ^{232}Th and ^{238}U (data from ENDF/B-VIII.0).

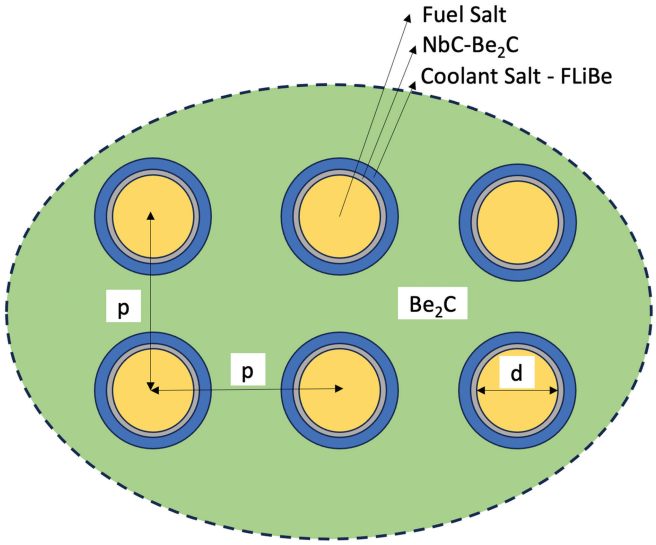

Fig. 3. Conceptual, partial horizontal MSBR core cross section showing general material configuration.

Additionally, the same FLiBe salt serves as the carrier base for the fuel salt in which ^{232}Th and uranium are dissolved.

Beryllium carbide (Be_2C) provides efficient moderation. The inclusion of beryllium in the moderator also somewhat improves the neutronic efficiency due to additional neutron production via the (n,2n) reaction with energetic neutrons. However, the benefit of beryllium is reduced by its (n,α) cross section, which produces ^{6}Li (a strong neutron absorber).[12]

Further discussions on the material selection and temperature-radiation compatibility are provided in Sec. III.F. The initial design employs a square lattice, i.e., with the same pitch p in the vertical and horizontal directions, and the same configuration for all fuel structures with constant diameter d for all fuel channels.

Uranium-233 has the highest neutron yield per neutron absorbed of any isotope for thermal-spectrum neutrons. The neutron yield per absorbed neutron for both ^{235}U and ^{239}Pu is insufficiently high to enable significant breeding with thermal-energy neutrons. The reproduction factor for each of these isotopes is graphically presented in Fig. 4. While the reproduction factor is roughly 2 for fully thermalized neutrons (~90 meV at fuel-salt temperatures) for both ^{235}U and ^{239}Pu, TS-MSRs have significant portions of their neutron flux that are not fully thermalized.[13]

To keep the attractiveness of the nuclear fuel low, ^{233}U needs to be bred in the presence of nonfissile uranium, which is challenging due to the high neutron capture cross section of ^{233}Pa. Hence, in the proposed fuel cycle, the fuel salt would frequently be removed from the critical circuit to minimize parasitic capture in ^{233}Pa. The model described here employs batch operation, in which a single batch of fuel salt is employed in the fuel-salt circuit, while the remainder of the batches are being processed out of the core to strip out the fission products and to allow ^{233}Pa to decay into ^{233}U. However, fuel salt could also be continuously removed and processed at an equivalent rate. Liquid fuel can readily be transferred from an active circuit without employing a salt-wetted valve using a goose neck–type lower connection and gas pressure–driven transfer.

A conceptual TS-MSBR vertical vessel and core cross section is shown Fig. 5. The fuel-salt volume is minimized (as compared to an open-core, loop-type MSR design) by configuring the fuel salt as a natural

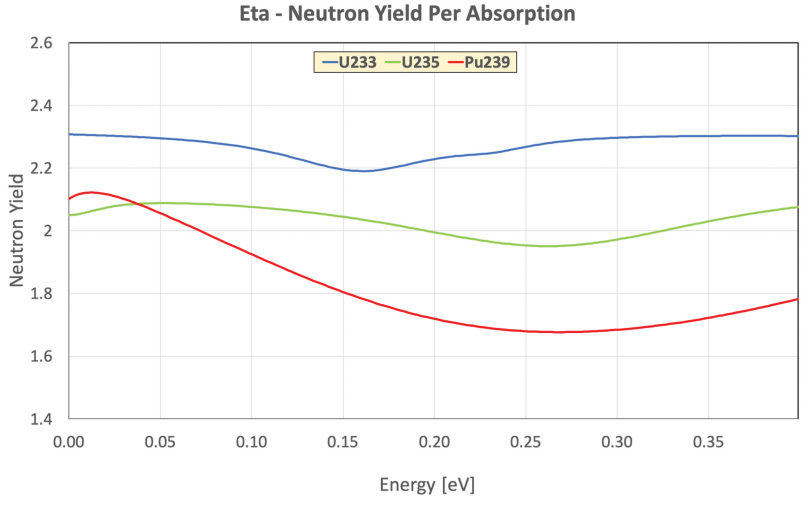

Fig. 4. Neutron yield per absorption for ^{233}U, ^{235}U, and ^{239}Pu in the thermal region (data from ENDF/B-VIII.0).

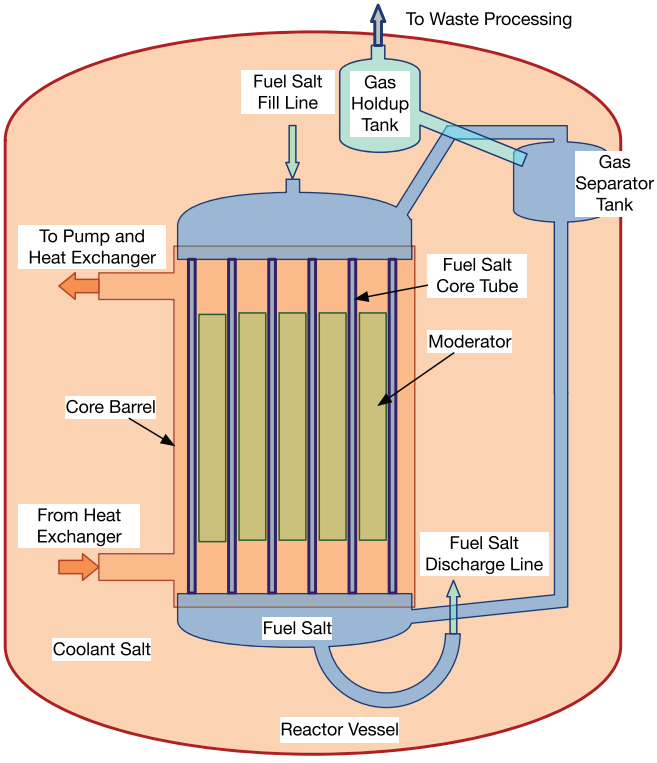

Fig. 5. Conceptual vertical reactor vessel and core section.

convection loop (with parallel legs) within the reactor vessel. The fuel-salt tubes are connected above and below the critical region to the inlet and outlet plenums.

The fuel salt flows via natural circulation within the fuel-salt circuit. The fuel-salt temperature increases as it flows upward in the core and decreases as it flows down the outside of the core (downcomer region). A gas separation system is included in the return line of the fuel salt. Throughout the circuit, the fuel salt is cooled by pumped coolant salt that enters the core barrel near the bottom and flows up through the core before exiting the core barrel near its top.

The fuel and coolant configuration (including employing a mix of ^{233}U and ^{238}U in the fuel salt) is conceptually similar to the Molten Salt Experimental (MOSEL) reactor concept studied in the 1960s.[14] However, the MOSEL concept employed a breeding blanket for its coolant salt, which would result in material that is more attractive than LEU. In the proposed design, fission gases (especially ^{135}Xe) are separated from the liquid fuel salt via a liquid-gas separator tank (likely via ultrasonic degassing)[15] that is also submerged in the coolant salt within the upper plenum of the reactor vessel. Fission gases are removed from the liquid-gas separator through extended tubing (to provide multiday residence time) within the coolant salt (e.g., helical coil heat exchanger). The overall fuel process steps are illustrated in Fig. 6.

A color-coded list providing additional information on the fuel processing steps shown in Fig. 6 is provided here:

1. (blue) Fuel-salt flows, under natural circulation (few cm/s), through a loop within the reactor vessel. The upward flow portion of the loop is subdivided into multiple individual tubes. The coolant salt and moderator surround each tube to create the core. Downflow is outside the core in an unmoderated downcomer region.

2. (orange) Fission gases are stripped from the fuel salt by a liquid-gas separator above the core submerged in coolant salt.

3. (black) Used fuel salt is removed from the critical loop and replaced by freshly processed fuel salt sufficiently frequently (every few weeks) to minimize parasitic absorption.

4. (black) Actinides are co-separated and removed from used fuel salt into aluminum, resulting in an (red) actinide-aluminum alloy and (green) carrier salt containing fission and activation products.[16]

5. (red) Actinides are stripped from aluminum-actinide alloy into actinide-chloride salt.[17–20]

6. (red) Actinide-chloride salt is converted to a fluoride fuel-salt concentrate.[21]

7. (red) Reconstituted fluoride fuel-salt concentrate is aged for several ^{233}Pa half-lives (~4 to 6 months).

8. (red) Additional fertile material is added (Th to breed and U_{nat} to denature) to the fuel-salt concentrate.

9. (orange) Fission products (green) are stripped from the used carrier salt to produce clean carrier salt to generate a (orange) stable fission product waste form.[22–24]

10. (black) The cleaned carrier salt is recycled by mixing with (red) fuel-salt concentrate, (black) which avoids creating a radioactive waste stream.

11. (blue) Fresh fuel salt is reintroduced into critical circuit (as described previously).

The total volume of fuel salt on site depends on the rate of barren fuel-salt reconditioning. Once the fission and contamination products have been stripped, the resultant carrier salt will be reused to synthesize fuel salt. If the reconditioning takes less than a single batch run time,

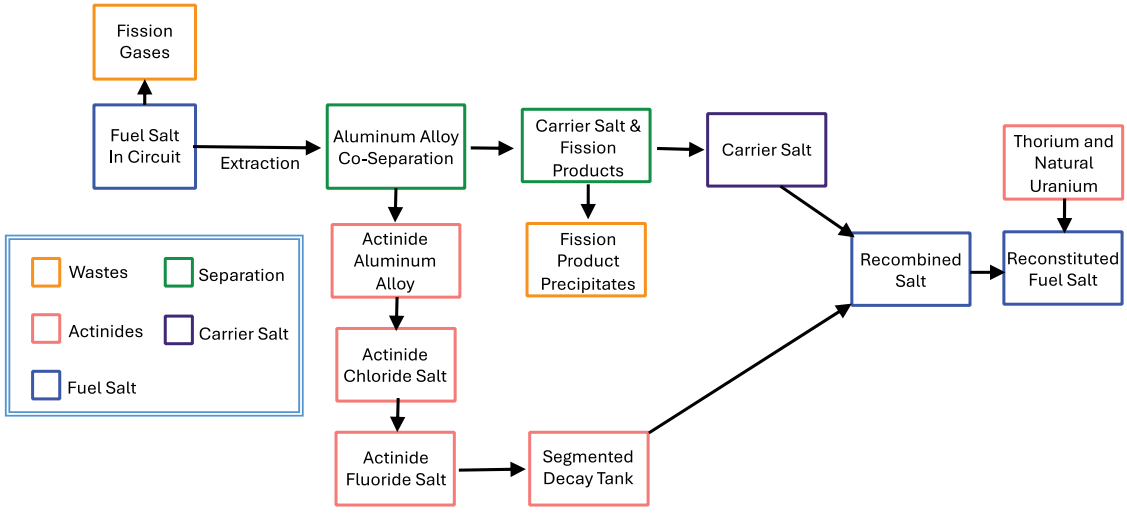

Fig. 6. Overall fuel process steps.

only sufficient carrier salt to fill the fuel-salt circuit two to three times will need to be on site. The proposed design becomes feasible only if the reactor can be kept critical with a large reactivity margin and if the fuel cycle can effectively support the transition from ^{235}U to ^{233}U operation. These points are addressed in the following section.

III.C. Reactor Conceptual Engineering Design and Optimization

The thicknesses of the structural casing tube and that of the coolant salt channel must be set to perform reactor cell optimization to determine the optimal fuel channel diameter and pitch. A summary of this analysis is presented in the following paragraphs.

The minimum thickness for the casing is set for it to be able to resist differential pressures in the internal fuel salt and the coolant salt. The maximum thickness of the casing is set to avoid generating unallowably large mechanical stresses due to the temperature profile developed across the casing by heat conduction from the fuel salt into the coolant salt. Although NbC-Be_2C is a brittle ceramic material, it can be fiber-reinforced similarly to other composites.[25] Hence, for computing the minimum thickness, we implemented the American Society of Mechanical Engineers standard ASME B31.3-2018 design for steel pipes with conservative safety factors. In this design method, the minimum thickness of the pipe is determined as follows:

$$t_{min} = \frac{PD_o}{2(SEW + PY)} \quad , \tag{1}$$

where

P = internal service overpressure, assumed to be a maximum of 0.3 MPa

D_o = pipe outside diameter

S = maximum allowable stress, conservatively taken as 50% of the tensile stress

E = a quality factor, conservatively assumed to be 0.8

W = weld joint strength reduction, conservatively assumed to be 0.5

Y = strength reduction coefficient, conservatively assumed to be 0.4.

The maximum thickness of the pipe is computed by solving heat conduction in the pipe with fixed Direchlet boundary conditions in the internal and external faces, computing the resulting equivalent Von Mises stress profile in the pipe, and equating the maximum stress to the maximum allowable stress in the pipe S. The resulting expression reads as follows:

$$t_{max} = \frac{D_i}{2}\left(e^{\frac{2\pi kS}{\alpha E_Y Q'}} - 1\right) \quad , \tag{2}$$

where

D_i = internal diameter

k = thermal conductivity

α = linear thermal expansion coefficient

E_Y = Young's modulus

Q' = linear heat generation rate.

The minimum and maximum pipe thicknesses, with the maximum pipe thinness computed for two prototypic linear heat generation rates, are depicted in Fig. 7. A pipe thickness of 2.54 mm was selected as it will allow for conservatively satisfying the mechanical constraints without introducing significant parasitic neutron absorption.

The thickness of the coolant salt annular t_c pipes was designed to maintain a reasonable pressure drop over the core, seeking to obtain the minimum possible diameter to avoid parasitic neutron absorptions. The linear pressure drop for the annular pipes of the coolant salt channels can be computed via the Fanning friction factors as follows:

$$\frac{\Delta p}{L} = \rho u^2 f(\mathrm{Re}) \frac{D_o + t_c}{\left(\frac{D_o}{2} + t_c\right)^2 - \left(\frac{D_o}{2}\right)^2} \quad , \tag{3}$$

where

Δp = pressure drop

L = length of the coolant pipes across the core

ρ = coolant density

u = prototypic coolant velocity

$f(\mathrm{Re})$ = Fanning friction factor as a function of the Reynolds number (Re), which is computed via the Colebrook-White correlation in this case.

The linear pressure drop for three different coolant prototypic velocities is shown in Fig. 8 assuming thermophysical properties for FLiBe with a constant temperature of 900 K. We selected a coolant channel thickness of 1 cm as it was the smallest value that introduced a reasonable pressure drop.

Once the thickness of the casing and the coolant pipe are fixed, the next step is the optimization of the reactor lattice configuration. For this purpose, version 14.0 of the OpenMC code was used, and a constant temperature of 900 K was assumed for all components in the lattice. For this optimization process, the fuel salt operates in its fresh fuel configuration, i.e., the fuel salt is a FLiBe base with 5% of dissolved ^{232}Th and 5.5% of dissolved LEU with 5 wt% ^{235}U.

Fresh fuel employs sufficiently isotopically separated lithium (99% ^{7}Li) to minimize its reactivity impact. The fresh fuel-salt composition in mole percent is 59.7LiF-29.8BeF_2-5ThF_4-5.5UF_4. The study was performed by varying the diameter and pitch distance between the fuel rods. The results of the study are presented in Fig. 9, where the infinite multiplication factor is studied as a function of the diameter of the fuel-salt channels and the difference between the pitch and the diameter. The highest infinite multiplication factors were obtained for a range of fuel rod diameters between 5 cm and 8 cm and a difference between pitch and diameter between 7 cm and 9 cm.

To be able to appropriately cool the fuel salt, we chose the minimum diameter in this range for the fuel-salt channel, which was 5 cm. Then, for a fuel-salt channel diameter of 5 cm, the maximum effective multiplication factor was obtained for a difference of pitch and diameter of 8 cm, i.e., for a pitch between fuel rod channels of 13 cm. The resulting spectrum for this optimized lattice configuration is shown in Fig. 10. As previously observed, the reactor maintains criticality with a thermal neutron spectrum with the flux peaking at around 100 meV.

The next step is determining the optimal dimensions for the reactor core. A parametric study was performed to find the optimal height and diameter of the reactor core

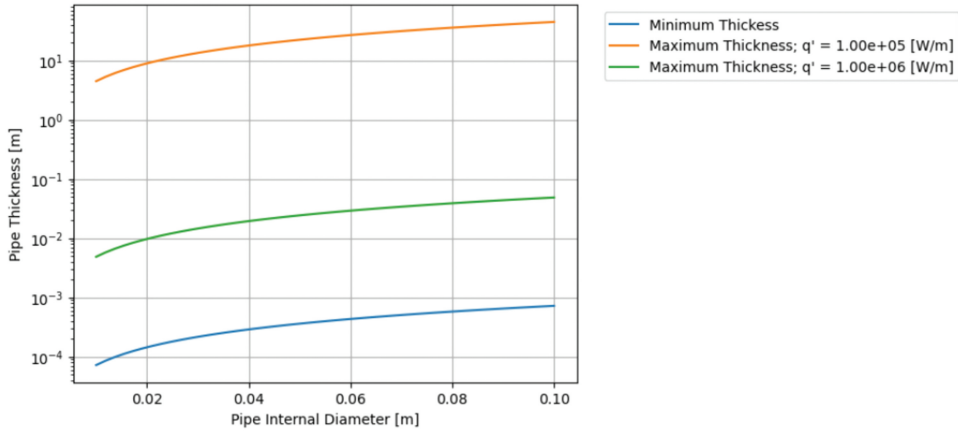

Fig. 7. Minimum and maximum thicknesses for the NbC-Be_2C casing pipes for two prototypic linear heat generation rates.

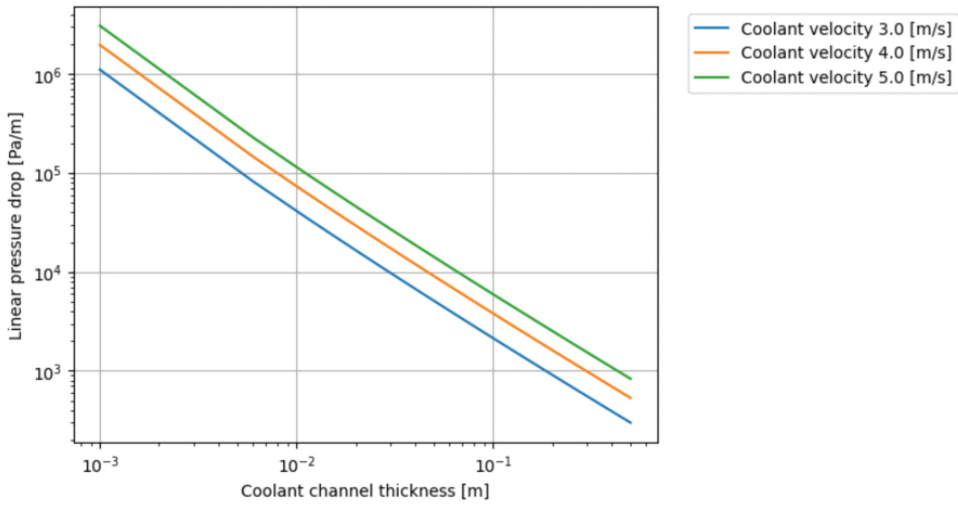

Fig. 8. Linear pressure drop for different coolant flow velocities.

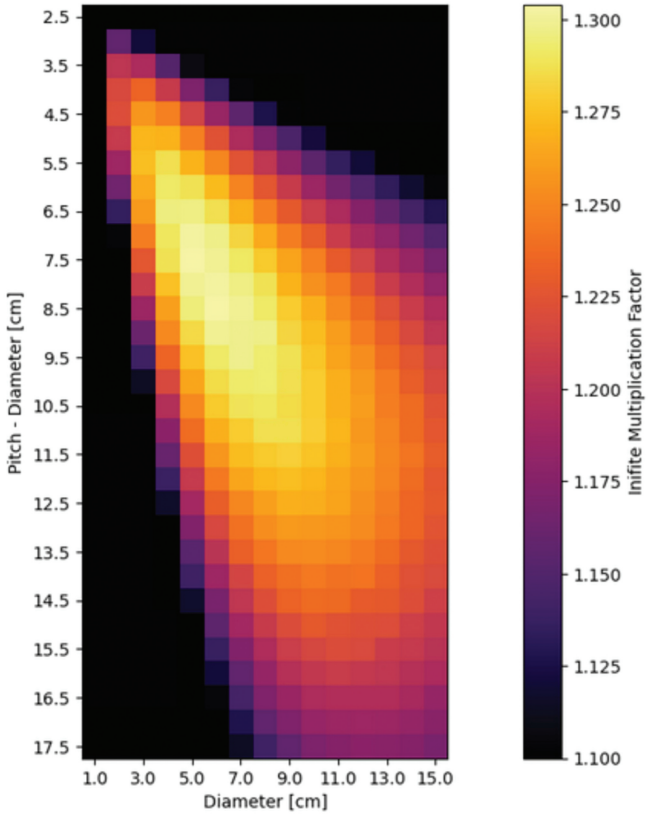

Fig. 9. Variation of the infinite multiplication factor as a function of the diameter of the fuel-salt channels and the difference between the pitch and the diameter of the fuel channels. The minimum value of the infinite multiplication factor has been limited to 1.1 for visualization purposes.

that guarantees operability via a sufficiently high effective multiplication factor. In this preliminary study, the core was designed with a square cylinder configuration, i.e., equal diameter and height. Additionally, the maximum reflector external thickness was limited to 0.5 m. The optimization study yielded a reactor that was 1.5 m in diameter and height and that had a fresh core effective multiplication factor of 1.075. Note that this effective multiplication factor is large enough to keep the reactor critical with fission product buildup during batch operation. Moreover, this multiplication factor is small enough to keep the reactor controllable during operation.

Once the neutronics of the reactor were optimized, the next step is the conceptual design of the reactor core to ensure the ability to transfer nuclear heat while only experiencing reasonable thermomechanical stresses. For this purpose, the volumetric heat generation rates computed by OpenMC were imported into the STAR-CCM+ multiphysics computational fluid dynamics software version 2022.1. The core thermal hydraulics and thermomechanics were then evaluated for steady-state operation at 300 MW(thermal). The effective core power density (i.e., power per total volume of the active core region) was 113 MW(thermal)/m^3, neglecting the external reflector.

The computational model of the reactor core is depicted in Fig. 11. The reactor core is composed by four main systems:

1. The fuel-salt circuit in which the fuel salt circulates upward in the reactor core driven by natural convection and then into a return pipe that links the top and bottom plena of the fuel-salt circuit. Additional cooling in the return pipe is introduced to drive natural convection.

2. The coolant circuit, for which only the section in immediate contact with the reactor core is studied. In this circuit, the coolant salt is pumped into a lower plenum by

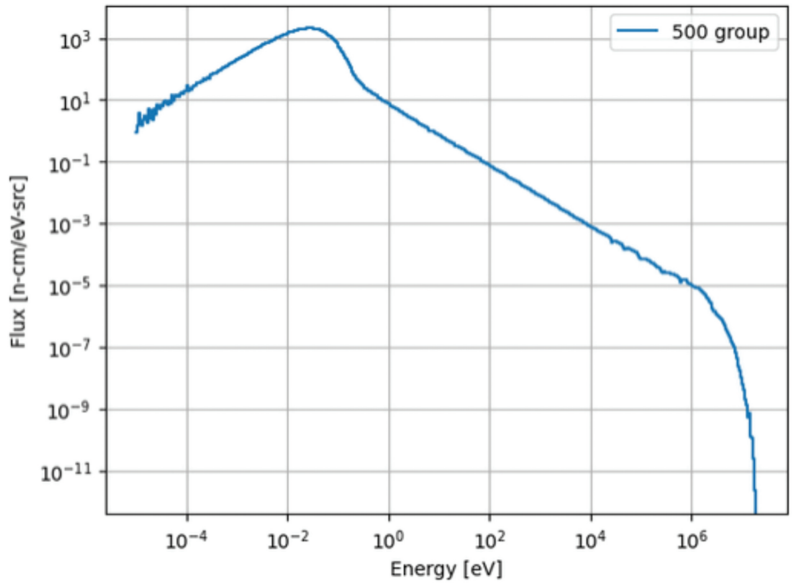

Fig. 10. Normalized 500-group resolved reactor spectrum for the optimized lattice configuration.

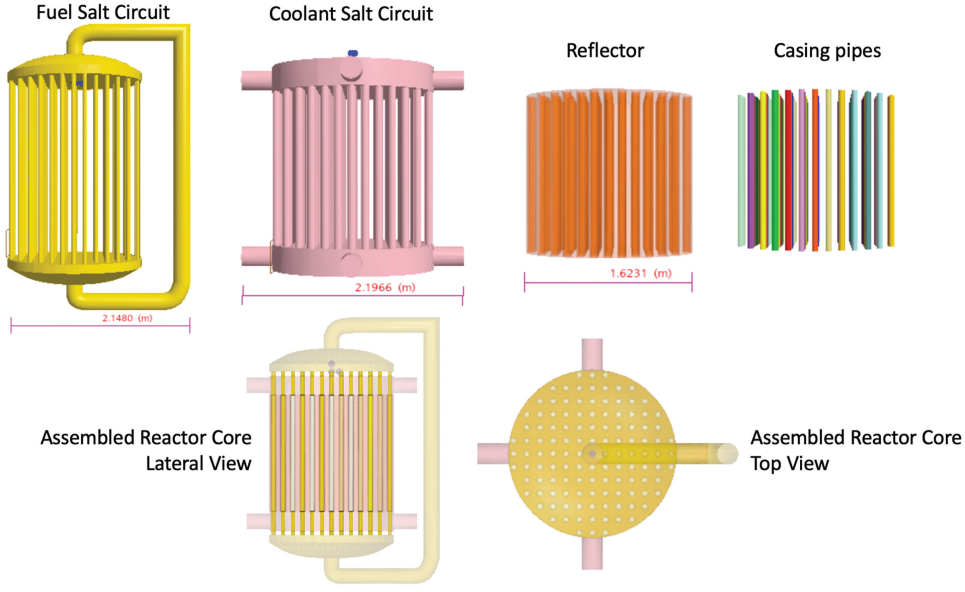

Fig. 11. Reactor configuration for computational fluid mechanics and computational thermomechanical studies. The top panels show the individual components of the reactor system, i.e., the fuel-salt circuit, the truncated coolant salt circuit, the neutron reflector, and the casing pipes of each fuel channel. The bottom panels show a lateral and top view of the assembled reactor configuration.

means of four inlets, and then the coolant salt circulates upward in the reactor core toward the top plenum, where it exits the reactor core by means of four outlet pipes.

3. The reflector, which surrounds the coolant pipes.

4. The casing pipes that separate the fuel and the coolant salt channels. The casing pipes are held by a top plate of NbC-Be_2C which is 12.7 mm thick and attached to the top plate of the neutron reflector. This holder plate has been purposely omitted in Fig. 11 to simplify the visualization.

The assembling of these systems is also shown in the bottom panel of Fig. 11. The reactor core assembly is shown in Fig. 3. Each unit cell, from the center toward the outer reflector, is composed of a fuel pipe, a casing

pipe, and surrounding reflector. A coolant annulus is formed between the reflector and the casing pipe. The outlets of the coolant salt circuit are via the coolant salt plena located above and below the neutron reflector. This design choice forces the plena of the fuel-salt system to be placed above the plena of the coolant salt system. The length of the piping in the fuel-salt circuit is large enough to achieve a considerable amount of natural convection, while minimizing the fuel-salt inventory needed for operation.

The temperature field and circulation velocity in the fuel salt during steady-state operation are shown in Fig. 12. The fuel salt circulates upward in the core and heats up due to the nuclear power deposition. Then it circulates from the top to the bottom plenum via the return pipe. A circulation velocity of ~0.8 m/s is achieved at the return pipe, while a velocity of ~0.05 m/s is obtained at the fuel-salt channels in the reactor core. Although small at the core, these natural circulation velocities are large enough to avoid getting unreasonably high temperatures at the core. The maximum temperature obtained toward the top of the fuel-salt channels is 1147.2 K, which is well within the acceptable bounds for the temperature of the fuel salt.

The temperature field, circulation velocity, and gauge pressure relative to the outlet pressure for the coolant salt are shown in Fig. 13. The coolant salt is forced into the four inlets in the bottom plena and then circulates upward in the coolant salt pipes at the core. A prototypic inlet velocity of 4 m/s was considered in this study. The temperature increases in the coolant salt pipes as it rises through the core channels. A reasonably good temperature mixing is then achieved in the top plenum, which leads to approximately uniform outlet temperatures. The fuel-salt temperature rise across the core was ~245 K, while the coolant salt temperature rise was ~40 K with a mixed mean coolant outlet temperature of 667°C. Finally, a total pressure drop of ~60 kPa was achieved by the coolant salt between inlet and outlet, which is in good agreement with the empirical studies presented in Fig. 8.

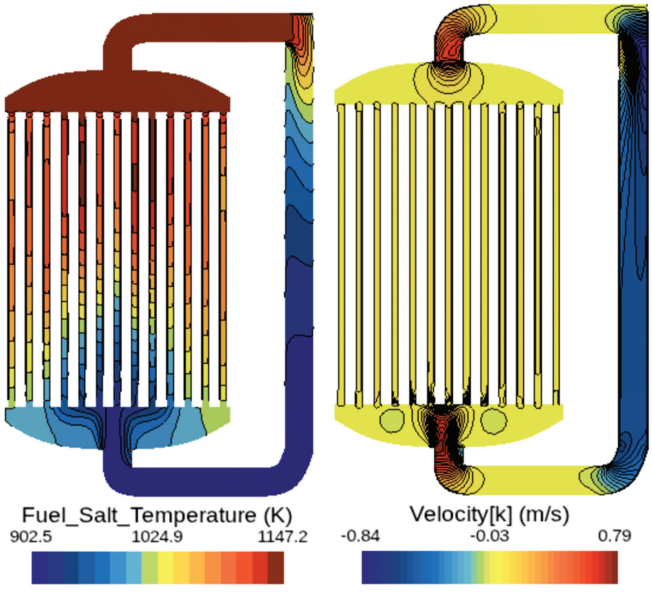

Fig. 12. Contour plots of key operation variables for the fuel-salt circuit shown at a vertical cut: (left) fuel-salt operating temperature and (right) fuel-salt vertical velocity.

The contour plots for the temperature field, equivalent stress field, and displacement magnitude field for the reflector and encasing pipe system are depicted in Fig. 14. The temperature field in the encasing pipes closely follows the temperature profile of the fuel salt. The Von Mises stress is maximal toward the top part of the reflector, where the holder plate for the encasing pipes is placed. To avoid mechanical compatibility issues during deformation, the outer surface of this plate is clamped, leading to larger stresses in this region. Nonetheless, the maximum Von Mises stresses obtained were below the tensile strength of Be_2C and NbC-Be_2C. Further mechanical optimization could be made to reduce this maximum stress.

Finally, relative displacements of ~2% were obtained toward the bottom region of the reflector and casing pipes. The larger displacements in this region were due to the unconstrained expansion of the reflector and pipes in this region. No geometrical compatibility issues were observed during the deformation process.

In summary, this subsection introduced a conceptual design for a TS-MSBR. Based on reasonable bounds for the casing pipe and coolant salt channel thickness, the reactor lattice was optimized for a fresh fuel configuration. Then full-core calculations were performed to determine the size of the core. Finally, thermal-hydraulic and thermomechanical studies were performed to propose an operational reactor concept that contains reasonable operational temperatures, pressure drops, mechanical stresses, and displacements.

With this reactor concept set, the next step is to demonstrate how a transition from ^{235}U-based to ^{233}U-based operation can be carried out in this reactor. This fuel cycle optimization is presented in the following subsection.

III.D. Preliminary Results for Optimized Fuel Cycle

The TS-MSBR starts operation with LEU with 5 wt% ^{235}U. The initial composition of LEU and

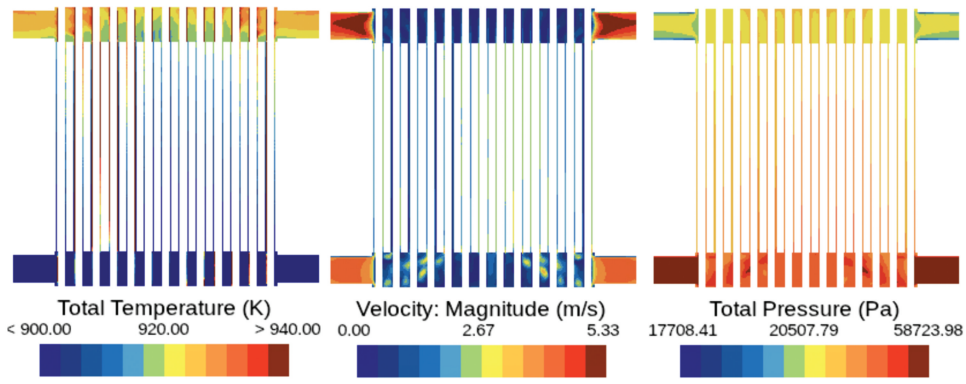

Fig. 13. Contour plots of key operation variables for the coolant salt circuit shown at a vertical cut: (left) coolant salt operating temperature, (center) coolant salt vertical velocity, and (right) coolant salt gauge pressure relative to outlet.

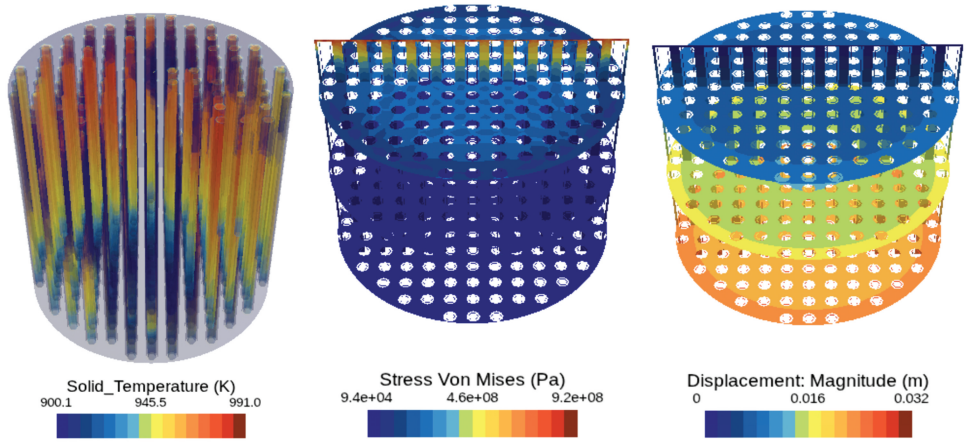

Fig. 14. Contour plots of key operation variables for the reflector and the encasing pipes system: (left) operating temperature, (center) Von Mises equivalent stress, and (right) displacement magnitude.

^{232}Th dissolved in the fuel salt was optimized to obtain a large effective multiplication factor, while having a small concentration of LEU and ^{232}Th to avoid excessively raising the melting temperature. As previously described, the reactor operates in a batch configuration. This operation is schematically shown in Fig. 15. The fuel-salt batch operates in the active fuel-salt circuit, and then is hydraulically transferred to the salt processing unit where the actinides and fission products are extracted. Finally, the actinides from the fuel batch go to local storage, where the bred ^{233}Pa is left to decay to ^{233}U. Once enough ^{233}U has been produced, the resultant actinide mixture is synthesized into fuel salt for reuse.

The time that each batch remains both inside the active fuel-salt circuit and outside of a high flux neutron region has been optimized to maximize ^{233}U production while minimizing parasitic neutron capture in ^{233}Pa under a constraint of avoiding a prohibitively large number of batches. The optimization was performed assuming a constant power density of 50 W/gram of heavy metals. The final configuration operates with six batches (one in use and five undergoing decay). The residence time at the core of each batch is 18.4 days, and the decay time outside of the core is 92 days.

Used liquid fuel salt could alternatively be continuously removed from the active loop along with the return of an equivalent amount of freshly processed fuel salt. This configuration yields a 95% ^{233}U yield when compared to the amount that would have been produced if no ^{233}Th or ^{233}Pa were consumed during reactor operation.

Once the batch operation has been optimized, the next step is to manage the Th and U inventory in the reactor core for three sequential purposes. The first operational goal is to transition from ^{235}U-based operation to criticality primarily with ^{233}U. Following the transition, the next goal is to maximize breeding new fuel while maintaining criticality by optimizing the Th to U ratio. Finally, for long-term operation, as new ^{233}U is produced

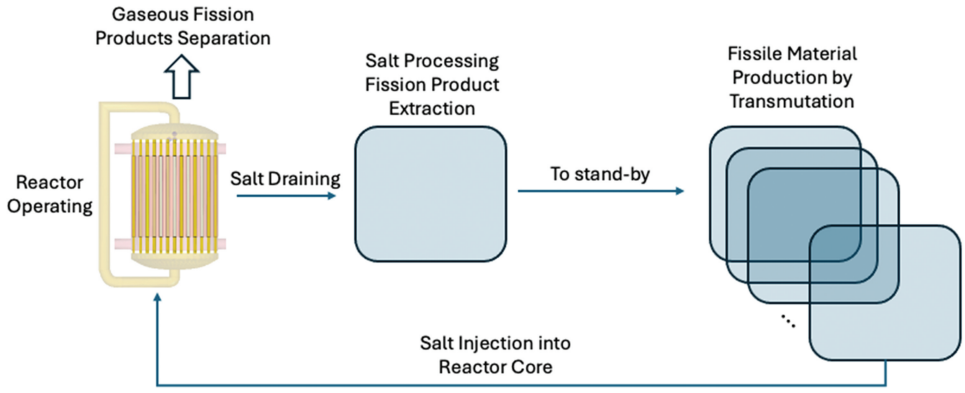

Fig. 15. Design of fissile material batch operation for the thermal breeding cycle of the TS-MSBR.

and ^{238}U is consumed, the fissile fraction of uranium in the core needs to be restricted to avoid developing an unacceptably attractive fissile isotope fraction. Each of the stages is addressed sequentially.

To achieve the first operational goal, different initial compositions of LEU and ^{232}Th were tried. However, none of these compositions achieved the desired conversion while keeping the reactor critical during the conversion. However, a successful transition could be obtained by actively controlling the amount of both LEU and ^{232}Th in the fuel salt while out of the core between batches. This actinide content management strategy resulted in a reactivity control being driven mainly by ^{232}Th, yielding a swift transition to ^{233}U-based operation.

The changes in the required quantities of ^{232}Th and LEU needed to keep the reactor critical over time are complex. The main reason for the complex shape is the time lag between the introduction of ^{232}Th and the effective reactivity rise by its conversion to ^{233}U. For this purpose, a proportional, integral, derivative (PID) actinide controller was defined to set the injection rates of ^{232}Th and LEU. The controller operates according to the following equation:

$$
\begin{aligned}
j_{\mathrm{Th}} &= K_P^{\mathrm{Th}}\left(k_{eff}-k_{sp}\right) + K_I^{\mathrm{Th},st}\frac{\int_{t_0}^{t_i}\left[k_{eff}(t)-k_{sp}(t)\right]dt}{(t_i-t_0)} \\
&\quad + K_I^{\mathrm{Th},lt}\int_0^{t_i}\left[k_{eff}(t)-k_{sp}(t)\right]dt \\
&\quad + K_D^{\mathrm{Th}}\frac{\left[k_{eff}(t_i)-k_{sp}(t_i)\right]-\left[k_{eff}(t_{i-1})-k_{sp}(t_{i-1})\right]}{t_i-t_{i-1}}\,, \\
j_{\mathrm{LEU}} &= -K_P^{\mathrm{LEU}}\left(k_{eff}-k_{sp}\right) - K_I^{\mathrm{LEU},lt}\int_0^{t_i}\left[k_{eff}(t)-k_{sp}(t)\right]dt \\
&\quad - K_D^{\mathrm{LEU}}\frac{\left[k_{eff}(t_i)-k_{sp}(t_i)\right]-\left[k_{eff}(t_{i-1})-k_{sp}(t_{i-1})\right]}{t_i-t_{i-1}}\,,
\end{aligned}
\tag{4}
$$

where

K_P^X, $K_I^{X,st}$, $K_I^{X,lt}$, K_D^X = proportional, short-term integral, long-term integral, and differential control constant for current X, with X being ^{232}Th or LEU

k_{eff} = effective multiplication factor

k_{sp} = set point multiplication factor, which is set to 1.03 as a target

t_i = time for the current batch

t_{i-1} = time of the previous batch

t_0 = time of five batches in the past.

The two-scale integral control is key for being able to deal with the time lag in the effective multiplication factor evolution introduced by ^{232}Th into the system. For the LEU addition, only long-term control was necessary. The values for the PID controller were found by using the root locus method, and were as follows:

$$
\begin{aligned}
&K_P^{\mathrm{Th}} = 30.0,\ K_I^{\mathrm{Th},st} = 12.0,\ K_I^{\mathrm{Th},lt} = 0.9,\ K_D^{\mathrm{Th}} = 0.1 \\
&K_P^{\mathrm{LEU}} = 2.1, K_I^{\mathrm{LEU},lt} = 0.1,\ K_D^{\mathrm{LEU}} = 0.0\ .
\end{aligned}
\tag{5}
$$

Both the transition to primarily ^{233}U criticality and the transition to efficient breeding would be simpler and shorter if higher-assay uranium fuel LEU were to become available for startup fuel. If 19.9 wt% ^{235}U uranium were to be used, ^{238}U burnout could be avoided altogether. The need for thorium removal from the fuel salt can be avoided for ^{235}U starting enrichments over 7%. Overall, LEU+ ($5\% < {}^{235}\mathrm{U} < 10\%$) appears to be a useful compromise, decreasing the complexity of making the transition from

enriched to bred fissile material criticality, as well as decreasing the time needed to achieve efficient breeding, yet relying on a more easily available uranium enrichment.

Each of the first six batches of fuel salt starts with identical fresh fuel salt and is grouped together as fuel-salt batch group one. Fuel-salt batch group two includes material with a single salt processing cycle. The discharge composition of the actinides and ^{135}Xe in the first batch groups of fuel salt, starting with 5 wt% ^{235}U, are shown in Fig. 16. The volume of each batch of fuel salt is 1.29 m^3. The full-circuit fuel-salt power density is 233.1 MW/m^3.

Once the transition from ^{235}U-based operation to ^{233}U-based operation is achieved, the next step is to begin breeding new fuel. Optimizing this transition is also challenging because to maximize breeding, the ratio of Th to ^{233}U needs to be increased. However, adding large amounts of Th would result in a short-term decrease in reactivity and only a longer-term increase in reactivity as ^{233}U is bred in. Hence, the optimization of the reactor breeding is defined by controlling thorium injection and uranium extraction to as rapidly as possible arrive at an optimal breeding composition.

The evolution of the effective multiplication factor and the breeding ratio as a function of the ^{232}Th-to-^{233}U ratio are depicted in Fig. 17 for several concentrations of ^{233}U. As expected, the breeding ratio increases as the Th-to-^{233}U ratio increases, and the effective multiplication factor decreases with this ratio. The precomputed optimization targets are those that maximize the breeding ratio while keeping the reactor critical with adequate margin, i.e., with the effective multiplication factor above the dashed line in Fig. 17.

The two controllers for the breeding currents that are added during the breeding process have the following form:

$$j_{Th}^{breed} = K_P^{\mathrm{Th},breed}\left[\left(\frac{\mathrm{Th}}{^{233}\mathrm{U}}\right) - \left(\frac{\mathrm{Th}}{^{233}\mathrm{U}}\right)_{tgt}\right] + K_I^{\mathrm{Th},breed}\int_0^{t_i}\left[\left(\frac{\mathrm{Th}}{^{233}\mathrm{U}}\right)(t) - \left(\frac{\mathrm{Th}}{^{233}\mathrm{U}}\right)_{tgt}(t)\right]dt + K_D^{\mathrm{Th},breed}\frac{\left[\left(\frac{\mathrm{Th}}{^{233}\mathrm{U}}\right)(t_i) - \left(\frac{\mathrm{Th}}{^{233}\mathrm{U}}\right)_{tgt}(t_i)\right] - \left[\left(\frac{\mathrm{Th}}{^{233}\mathrm{U}}\right)(t_{i-1}) - \left(\frac{\mathrm{Th}}{^{233}\mathrm{U}}\right)_{tgt}(t_{i-1})\right]}{t_i - t_{i-1}} \tag{6a}$$

$$j_{\mathrm{U}}^{breed} = -K_P^{\mathrm{U},breed}\left[\left(\frac{\mathrm{Th}}{^{233}\mathrm{U}}\right) - \left(\frac{\mathrm{Th}}{^{233}\mathrm{U}}\right)_{tgt}\right] - K_I^{\mathrm{U},breed}\int_0^{t_i}\left[\left(\frac{\mathrm{Th}}{^{233}\mathrm{U}}\right)(t) - \left(\frac{\mathrm{Th}}{^{233}\mathrm{U}}\right)_{tgt}(t)\right]dt - K_D^{\mathrm{U},breed}\frac{\left[\left(\frac{\mathrm{Th}}{^{233}\mathrm{U}}\right)(t_i) - \left(\frac{\mathrm{Th}}{^{233}\mathrm{U}}\right)_{tgt}(t_i)\right] - \left[\left(\frac{\mathrm{Th}}{^{233}\mathrm{U}}\right)(t_{i-1}) - \left(\frac{\mathrm{Th}}{^{233}\mathrm{U}}\right)_{tgt}(t_{i-1})\right]}{t_i - t_{i-1}}, \tag{6b}$$

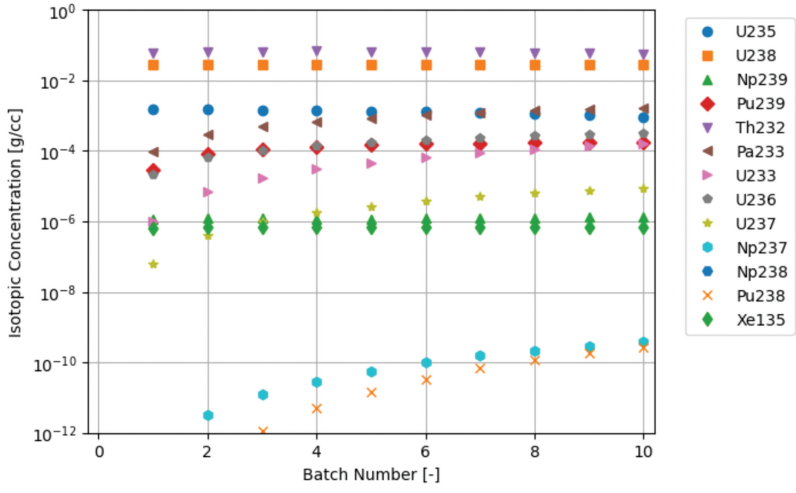

Fig. 16. Isotopic concentration of the first 10 cycles of one characteristic batch before operation in the reactor core when starting with 5 wt% of ^{235}U.

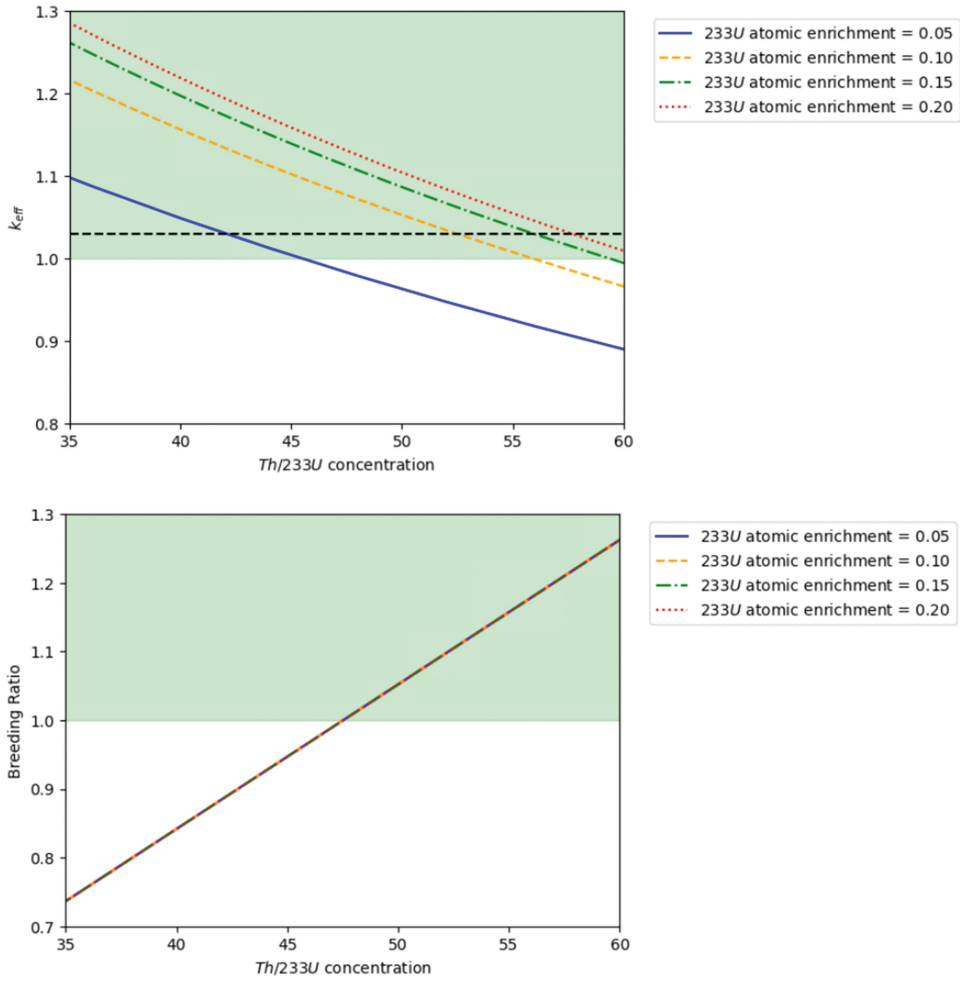

Fig. 17. (top) Evolution of the effective multiplication factor and (bottom) breeding ratio as a function of the Th-to-^{233}U ratio.

where $K_P^{X,breed}$, $K_I^{X,breed}$, and $K_D^{X,breed}$ are the proportional, integral, and differential control constant for current X, with X being Th or U. Note that the j_{Th}^{breed} current is injected to the in-use fuel salt, while the j_{U}^{breed} current is extracted from the in-use fuel salt with the concentration of uranium isotopes that has been produced in the in-use fuel salt after each batch operation. Additionally, $\left(\frac{\text{Th}}{^{233}\text{U}}\right)_{tgt}$ is the preoptimized Th to ^{233}U target, which is dynamically computed as a function of the uranium enrichment during the breeding cycle.

The proportionality constants of the midterm control system have been optimized to minimize the time to achieve the target breeding ratio and have the following values:

$$K_P^{\text{Th},breed} = 21.2, K_I^{\text{Th},breed} = 6.3, K_D^{\text{Th},breed} = 0.2$$
$$K_P^{\text{U},breed} = 3.1, K_I^{\text{U},breed} = 0.4, K_D^{\text{U},breed} = 0.0 \quad . \quad (7)$$

Note that the two control systems proposed in for the short term in Eq. (4), and for the midterm in Eq. (6), are incompatible in the long term as they will lead to an overcontrolled reactivity target. The short-term control is only used for the first 120 months to achieve the transition from ^{235}U-based to ^{233}U-based operation, while the mid-range control system is always activated. This results in a system that maximizes the breeding ratio, while keeping the reactivity controlled due to the dynamic optimization target.

Finally, long-term control is oriented to keeping the fissile content of uranium controlled. This is needed because when the reactor transitions to ^{233}U operation, no more LEU is added. Hence, ^{238}U keeps burning while ^{233}U keeps being produced, and therefore, the fissile fraction of the uranium mixture keeps increasing. The long-term control system consists of adding natural uranium to keep the fissile fraction of the uranium mixture below 19.9%. This control system reads as follows:

$$j_{\mathrm{U}}^{enr} = K_P^{\mathrm{U},enr} \min\left(\epsilon_{\mathrm{U}} - \epsilon_{U,max}, 0\right) + K_I^{\mathrm{U},enr} \int_0^{t_i} \min\left[\epsilon_{\mathrm{U}}(t) - \epsilon_{\mathrm{U},max}, 0\right] dt \quad , \tag{8}$$

where j_{U}^{enr} is the enrichment current of natural uranium, $K_P^{\mathrm{U},enr}$ and $K_I^{\mathrm{U},enr}$ are the proportional and integral control constants, and ϵ_{U} and $\epsilon_{\mathrm{U},max}$ are the current and maximum uranium enrichment. No differential control was needed for the long-term system. The optimized values of the control parameters are $K_P^{\mathrm{U},enr} = 0.044$ and $K_I^{\mathrm{U},enr} = 0.021$. During long-term operation, both the midterm and long-term control systems remain active.

The reactor effective neutron multiplication factor for a characteristic batch with the PID control system begins at 1.07, rapidly decreases to 1.03, and remains stable thereafter. As the batches are rotating through the reactor life cycle, a characteristic batch is simply the first batch that operates in the reactor core for 18.4 days and then decays out of the core for 92 days. The fission products are extracted from the fuel salt every 18.4 days, while the ^{135}Xe is actively removed during operation. The reactivity at each cycle is computed after this reprocessing stage.

The injected currents for LEU and ^{232}Th as optimized by the PID controller are depicted in Fig. 18. For short-term control, initially, a large amount ^{232}Th is inserted, which results in a more rapid buildup of ^{233}U to accelerate the transition into the Th-U fuel cycle. A small current of LEU is necessary to keep the reactor critical for approximately the first 100 months of operation. The requirement for this current is reduced by extracting ^{232}Th out of the system at later stages in the operation cycle. The gained reactivity by ^{232}Th extraction reduces the buildup of ^{238}U that would result in significantly higher concentrations of uranium and thorium at later stages of operation. Finally, when transitioning into longer-term operation, the stream of ^{232}Th increases to keep producing the ^{233}U that gets burned during operation.

The total mass of needed LEU per batch for the initial operation and refueling is 1231 kg, with 449 kg being loaded at the beginning of the operation and the remaining 782 kg used for refueling during the transition from ^{235}U-based to ^{233}U-based operation. Hence, the total amount of LEU needed for the plant to achieve transition is 7386 kg, which is about two-thirds (on a per kW(thermal) basis) of the around 90 tonne needed for the initial fuel load of a large pressurized water reactor (PWR) (which would require multiple reloads over the 100 months during which the TS-MSBR would require LEU supplementation).

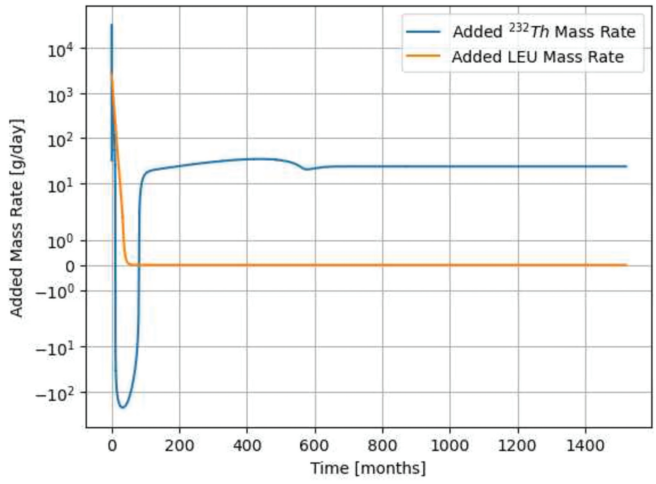

Fig. 18. Injected currents of (orange) LEU and (blue) ^{232}Th as optimized by the PID controller.

After 120 months, the midterm control system takes over. During midterm control, the Th injection current starts rising to achieve higher breeding ratios. During this time, most of the ^{233}U is kept in the core to allow for further Th injection. During this intermediate period, ^{233}U is bred from ^{232}Th, while ^{238}U keeps being burned in the fuel. This results in a progressively higher fissile fraction of the uranium in the reactor core. At ~550 months of operation, the fissile fraction of the uranium would surpass the allowed maximum of 19.9%. This activates the long-term reactivity control system, which adds natural uranium to the fuel salt. This addition results in a reactivity decrease that is compensated by reducing the injection rate of Th in the core.

The evolution of key isotopes over time is depicted in Fig. 19. For the initial 120 months of operation, the concentration of ^{232}Th is first increased and then reduced through periodic batch processing. The ^{235}U concentration slowly reduces while progressively smaller amounts of LEU are added into the system, and then rapidly reduces after the LEU addition ceases. By ~200 months of operation, virtually no more ^{235}U remains in the fuel salt. The amount of ^{238}U in the fuel salt is approximately constant while LEU is being added, and then reduces through depletion once LEU addition ceases. The amount of ^{233}U in the fuel salt progressively builds up, and by ~100 months, surpasses the concentration of ^{235}U.

When the midterm control activates after 120 months, the amount of ^{232}Th in the fuel salt is progressively increased. The higher concentration of ^{232}Th eventually results in a higher concentration of ^{233}U due to breeding. As the ^{233}U fraction increases, an increased concentration

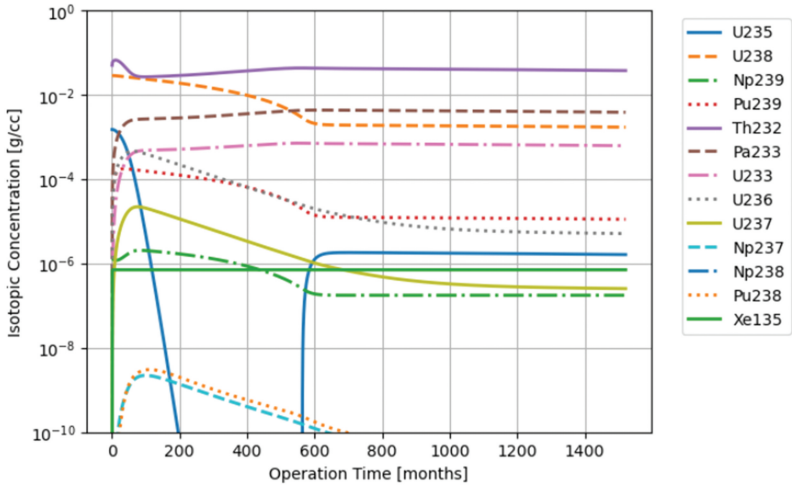

Fig. 19. Isotopic evolution of key isotopes during PID-controlled operation.

of ^{232}Th becomes possible, which maximizes the breeding ratio while keeping the reactor critical, as shown in Fig. 17.

At about 600 months, the fraction of ^{233}U reaches the fissile fraction limit of 19.9%. After this time, natural uranium is added along with the ^{232}Th to limit fissile material attractiveness. The natural uranium addition results in the stabilization of the ^{238}U concentration and the reintroduction of some ^{235}U to the fuel salt due to its presence in natural uranium. Additionally, as the fraction of ^{233}U in the uranium mixture is now fixed at 19.9%, the optimization target for the midterm control system is also fixed. This results in a constant, stable concentration for ^{232}Th and ^{233}U.

Two extra parameters are important to be controlled during the evolution of the compositions in the fuel salt. First, the concentration of Th and U must be kept low enough to avoid raising the fuel-salt melting temperature undesirably. The historic TS-MSBR program evaluated the properties of LiF-BeF_2-ThF_4-UF_4 salts and found that those with less than 20 mol % actinides maintained sufficiently low melting points and viscosities to be useful as fuel salts.[26] Second, the effective uranium enrichment, i.e., the ratio of fissile over nonfissile uranium, must be kept low to reduce the attractiveness of the fuel salt. The evolution of these two metrics during operation is presented in Fig. 20.

In the left panel of Fig. 20, we observe that the uranium concentration effectively reduces during operation. At the beginning of operation, this concentration reduces faster due to the faster burnup of ^{235}U. Then it reduces more slowly as a significant amount of ^{233}U is produced and ^{238}U is still slowly burned. The concentration of uranium reaches steady state once the isotopics are stabilized at ~600 months. The concentration of ^{232}Th increases initially due to the initial injection necessary to boost the production of ^{233}U. Nonetheless, the maximum concentration that ^{232}Th reaches is below 7%, which is significantly below the solubility limits for ^{232}Th in FLiBe. The concentration of ^{232}Th is then actively decreased during batch fuel salt processing to achieve the transition to ^{233}U while keeping the reactor critical, and then increases during midterm operation to maximize the breeding ratio.

The evolution of the effective uranium enrichment is shown in the right panel of Fig. 20. The enrichment reduces initially as ^{235}U burns and only small amounts of ^{233}U are produced. Steady reactivity (k_{eff} = 1.03) is achieved by balancing reducing the uranium concentration (left panel in Fig. 20) with increasing its fissile fraction (right panel in Fig. 20). For midrange operation, the enrichment of uranium rapidly increases as ^{233}U is produced with a growing concentration of ^{232}Th while the ^{238}U is being depleted. The uranium fissile fraction continues to increase until ~600 months, when the long-term control system starts the injection of the natural uranium.

Finally, the currents of extracted ^{233}U, ^{235}U, and ^{238}U by the midrange control system are plotted in Fig. 21. As observed in the figure, no significant extraction happens before ~120 months until the midrange control system takes over control. Then the current extracted from the core contains primarily ^{238}U and ^{233}U. The amount of extracted ^{238}U decreases and the one of ^{233}U increases as the enrichment in the fuel increases. Then, after ~600 months, the extraction rates reach a constant value as the isotope concentrations in the reactor go to equilibrium. The doubling time for the extracted fuel to reach the mass needed for a new batch is 709.3 months at the 120-month composition. Once the core reaches equilibrium, the doubling time reduces to 71.5 months.

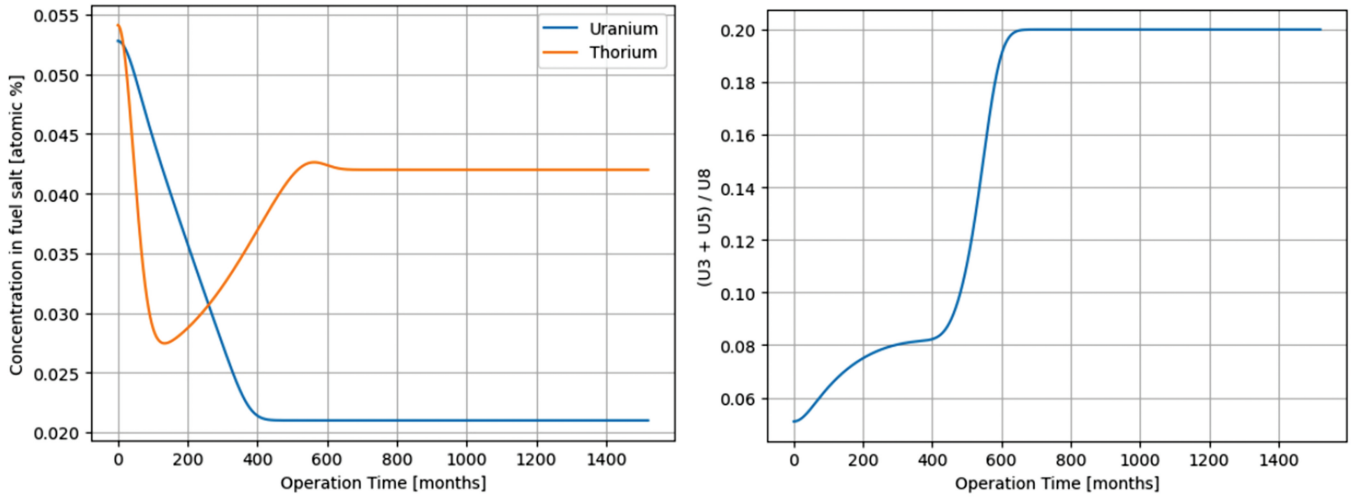

Fig. 20. (left) Evolution of the concentration of Th and U in the fuel salt and (right) uranium fissile content evolution.

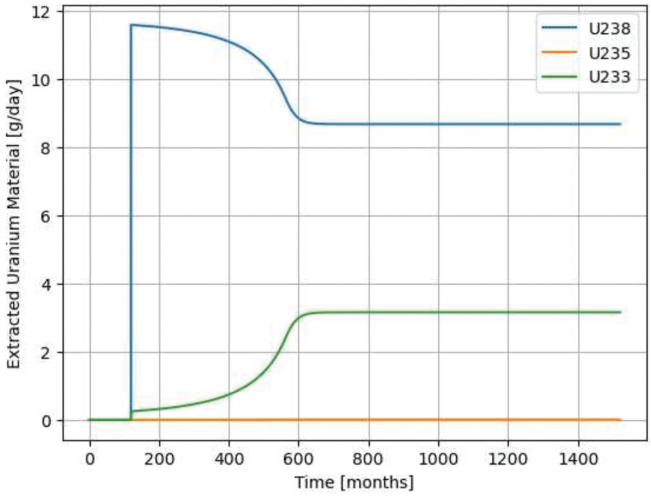

Fig. 21. Evolution of the extracted current of uranium over operation.

III.E. Proliferation-Resistant Processing

Denaturing and co-separation are the key technological elements to avoid creating material that is more attractive than LEU anywhere in the fuel cycle. The proposed liquid salt fuel incorporates a mixture of thorium and uranium. Thorium along with small quantities of natural uranium are its equilibrium feedstock materials. The fuel-salt uranium-isotopic blend at all times contains sufficient nonfissile ^{238}U to avoid generating material more attractive than LEU, i.e., the fuel salt is denatured.

While the United States does not have a definition of LEU that includes isotopes other then ^{235}U and ^{238}U, the International Atomic Energy Agency detection timeliness table, from its safeguards glossary,[27] indicates that isotopic mixtures of uranium containing a total of less than 20% of ^{233}U and ^{235}U remain at the highest conversion time interval.

Co-separation keeps the fissile and fertile isotopes of uranium together along with the other trivalent actinides (e.g., plutonium, americium, and protactinium) to avoid generating separated, attractive material. An additional feature in the proposed reactor design is that the total mass of ^{239}Pu during operation remains smaller than a significant quantity, as depicted in Fig. 22, and remains in extremely dilute form, as shown in Fig. 19.[27] Actinide extraction from the fuel salt enables the subsequent removal of fission product parasitic absorbers, both improving neutronic efficiency and maintaining fuel-salt thermophysical properties. Actinides can be co-separated from fluoride salt via reductive extraction into an aluminum alloy.[28,29]

While the aluminum alloy–based co-separation technology is thermodynamically favorable and has shown high actinide separation factors under laboratory conditions, the technology remains immature with substantial unknowns. For example, the distribution of thorium remains uncertain (thorium is less energetically favorable to remove).[30] While thorium has no fissile isotopes and its distribution does not impact the material attractiveness of the salt, understanding its separation characteristics remains an unresolved issue.

III.F. Materials

The envisioned reactor would be possible with traditional materials (i.e., with metal alloy tubes and graphite moderation). However, advanced materials would enable improved performance. In particular, reasonable

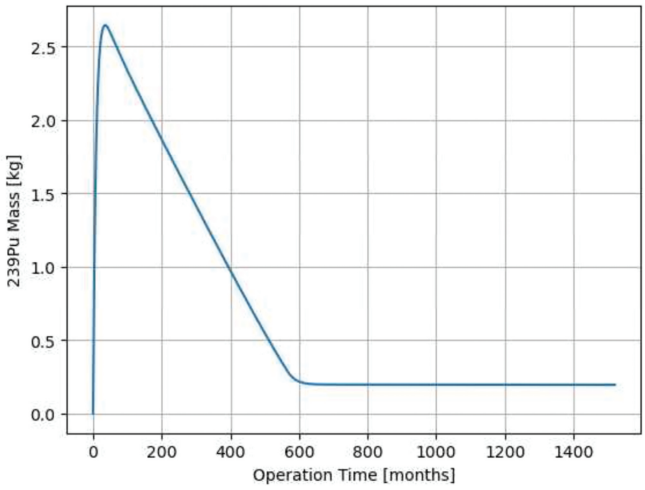

Fig. 22. Evolution of the inventory of ^{239}Pu in the fuel salt during operation.

thickness metal alloy tubes would absorb too many neutrons to maintain criticality employing only 5% ^{235}U fuel salt while the reactor transitions to ^{233}U operation.

Graphite is the only proven fuel salt–compatible moderator. Graphite, however, has both a limited displacement damage tolerance and is not a volumetrically efficient moderator. The neutron moderation length in carbon is over 60 cm versus under 6 cm in water.[31] Radiation damage to graphite has long been a known design issue for MSRs. Radiation damage to graphite was central to Oak Ridge National Laboratory's (ORNL's) decision in 1967 to shift from a dual to a single fluid MSR, and was a central rationale in halving the power density of the MSBR's conceptual design.[32,33] Additionally, graphite that has been exposed to fuel salt represents a significant contaminated waste stream.

An optimized core configuration would employ two alternative, advanced materials:

1. A coolant salt–compatible high-temperature moderator with high radiation damage tolerance

2. Fuel-salt tubes that are chemically compatible with both fuel and coolant salts and that have low neutron absorption, high radiation damage tolerance, and strength at high temperature.

Beryllium carbide has the potential to be the base material to achieve both objectives. Be_2C has an antifluorite crystal structure, the same crystalline configuration (with anions and cations reversed) as exceptionally radiation damage–resistant fluorite-type crystals (e.g., UO_2). A related antifluorite crystal (Li_2O) has also been shown to have high radiation damage tolerance.[34,35]

While the analogous material performance information provides a rationale for expending resources to assess the radiation damage characteristics of Be_2C, the radiation damage characteristics of Be_2C remain speculative with only low-displacement irradiations previously performed.[36–38] Be_2C does not activate substantially, but has multiple small cross-section, gas-generating threshold reactions (see Fig. 23). Consequently, Be_2C pieces exposed to energetic neutrons may need to be occasionally baked out over the course of the plant lifetime to remove gases that do not release at operating temperature but do migrate to form gas-stabilized voids.

The DOE Office of Nuclear Energy (NE) sponsored an early-phase ion beam–based Be_2C irradiation damage evaluation project in 2023.[39] However, further work remains necessary to adequately understand the radiation damage. If Be_2C exhibits desirable radiation damage characteristics, substantial further development would be recommended.

Beryllium carbide is vulnerable to hydrolysis. The native beryllium oxide coating on Be_2C is thermodynamically stable in FLiBe. Tritium dissolved in FLiBe coolant salt may react with the oxide to form beryllium hydroxide and methane gas.[40] Conversion of tritium into methane would be useful for MSRs, as tritium is the only radionuclide with significant potential to escape under normal operating conditions.

Beryllium carbide, however, does have usage limitations. Be_2C (like all carbides) is brittle and may require the use of ceramic toughing techniques. Bare Be_2C is not compatible with fuel salt, as uranium fluoride will react with it to form solid uranium carbide and beryllium metal. In general, Be_2C is also not thermodynamically stable at high temperatures against common structural materials (particularly in the presence of oxygen), but it is thermodynamically stable against clean FLiBe (^{2}LiF-BeF_2) salt. Be_2C is also stable in dry air up to nearly 1600°C due to the formation of an adherent oxide coating.[41]

Metal alloy fuel-salt tubes are possible, but would result in both a larger neutron absorption and a lower maximum temperature (due to decreasing alloy strength at high temperatures) and would be vulnerable to radiation-induced cracking (analogously to fuel cladding), necessitating undesirably frequent replacement.

Niobium carbide is thermodynamically stable against both UF_3 and UF_4. Moreover, niobium has an acceptably small neutron absorption cross section, and consequently, has been used as a component in LWR cladding[42] and has been evaluated as a material for nuclear thermal propulsion rocket engines, as well as fully ceramic

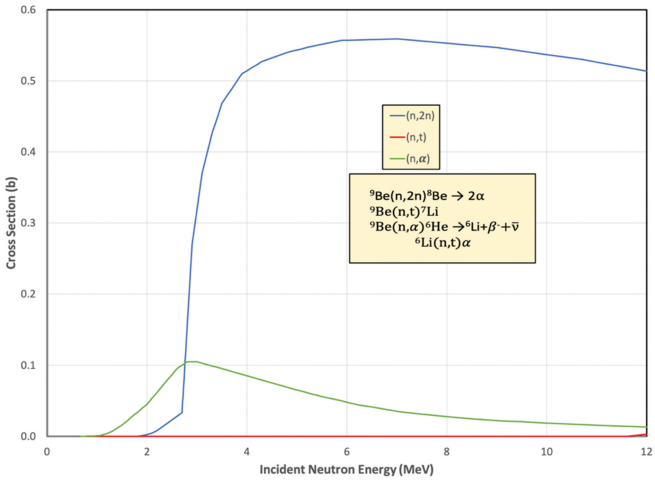

Fig. 23. Beryllium gas generating reactions (data from ENDF/B-VIII.0).

microencapsulated fuels.[43,44] Sintering aids are commonly used in powder metallurgy to decrease the time/temperature/pressure requirements to form dense compacts. Chemically activated sintering relies on a chemical reaction between the sintering aid at the bulk powder to bind the particles together. A survey of potential sintering aids for Be_2C was made in the 1950s stating:

> The general survey of bonding agents for beryllium carbide revealed no material which permitted fabrication of bodies having porosities of 10% or less at temperatures lower than those required to produce dense compacts of beryllium carbide per se. The one notable exception, however, was uranium carbide. Uranium-carbide additions facilitated the fabrication of dense beryllium-carbide compacts.[41]

The use of a sintering aid containing uranium carbide and aluminum resulted in the formation of a "network of uranium-bearing phase around the beryllium carbide grains."[41]

As niobium is an even stronger carbide former than uranium, it can substitute in forming a protective layer of niobium carbide enveloping and joining the Be_2C grains. The reaction of Nb with Be_2C is exothermic (10 Kcal/mol) providing the chemical energy to aid the sintering and form the protective, enveloping network. Niobium carbide is thermodynamically compatible with uranium-fluoride salts, so it would be immune from chemical attack. Also, the coefficients of thermal expansion of Be_2C and NbC are similar. Moreover, as the niobium carbide coating is developed at the grain level, mechanically damaging the resultant compacts primarily exposes an additional niobium carbide surface, maintaining corrosion resistance.

Using conventional powder metallurgy techniques, NbC-Be_2C appears likely to be formable via extrusion (into tubes) and would enable higher-temperature reactor operation. Extrusion lowers the sintering initiation temperature by mechanically forming fresh (chemically reactive) surfaces. Note, the ceramic-to-metal tube joints at the upper and lower tube bank plenums will be a key design issue. The joints would likely employ a set of thin-walled, hollow, metallic O-rings to provide the necessary compliance.

IV. MSBR TECHNICAL ISSUES (AS OF 1972)

A review by an independent, expert panel remains the best available method for assessing complex, interrelated technologies such as MSBRs. The technical issues required to be resolved prior to MSR commercial deployment were evaluated by the U.S. Atomic Energy Commission's Division of Reactor Development and Technology in 1972 and documented in WASH-1222.[45] The identified issues were the

1. Development and demonstration of an integrated fuel-salt processing system.
2. Development of suitable reactor and processing system structural materials.
3. Development of a satisfactory method for the control and retention of tritium.
4. Development of a more complete understanding of the physical/chemical characteristics of irradiated fuel salt, including the behavior of fission products.
5. Development of long-life moderator graphite suitable for breeder application.
6. Conceptual definition of the engineering features of the components and systems.
7. Development of adequate systems and equipment for remote inspection, handling, and maintenance
8. Codes and standards for high-temperature materials.
9. Demonstration of safety technology.

While the review is somewhat dated, is focused on the specific design elements of the historic MSBR, and occurred prior to proliferation resistance and safeguards becoming key fuel cycle elements, the topics identified

provide reasonable guidance on the necessary developments required prior to commercial MSBR deployment. The review also presumed a government-centric development process as opposed to a public-private partnership led by the needs of private developers, as would be anticipated today.

The current status along with a path toward the resolution of the remaining issues is provided in the following sections.

IV.A. Integrated Fuel-Salt Processing System

The development and demonstration of fuel-salt processing technology remains recommended as the technology development element with the largest remaining uncertainties. However, the historic MSBR program was planning to implement very chemically aggressive processes (fluorination to remove uranium followed by multiple stages of liquid-bismuth reductive extraction) to enable breeding.[46] Now, much less aggressive processing (e.g., contacting with an aluminum alloy followed by melt recrystallization) is anticipated.

IV.B. Reactor and Processing System Structural Materials

The reactor structural material issue was largely resolved by the development of fuel-salt redox control methods in the 1970s[47] and a lesson learned to include substantial shielding between high neutron fluxes and nickel-based alloys. Niobium carbide–bonded Be_2C offers the potential for an extremely durable core structural material. Much less chemically aggressive processing also substantially simplifies the processing system structural materials. Recent demonstrations of the capability of cathodic protection to provide corrosion protection in halide salts also expands the ability to use available alloys at MSRs.

IV.C. Control and Retention of Tritium

Beryllium carbide is a methanide and is sensitive to hydrolysis. In the presence of hydrogen and oxygen, it will break down into methane and beryllium hydroxide. Beryllium oxide will form as a stable oxide coating on Be_2C in FLiBe. Methane is readily trapped and does not diffuse through structural alloys. The use of Be_2C as a moderator material and as a tritium trap appears to be a practical solution and is recommended.

Tritium is formed as a dissolved gas in the fuel and coolant salts. While the purpose of the fuel-salt degassing system will be to remove ^{135}Xe, tritium will be induced to bubble out from the fuel salt. The coolant salt will likely also incorporate a degassing unit with the primary purpose to strip the tritium and/or methane into a head space where it can be chemically trapped.

IV.D. Development of a More Complete Understanding of Irradiated Fuel Salt and Fission Products

Developers and safety evaluators require an adequate understanding of irradiated fuel-salt properties. Improving the understanding of fuel-salt properties has been a central element of the modern DOE NE MSR campaign for the past few years, and a public molten salt property database has been created.[48] Current efforts are focused on expanding the database to include all relevant salts and continuing to improve the quality of the information in the database to minimize the conservatism necessary in reactor design and safety evaluations. Additional fuel-salt irradiations focused on understanding radioactive material releases into vapors and aerosols would be a useful element of a MSR safety evaluation program.

IV.E. Development of Long-Life Moderator Compatible with Fuel Salt

Niobium carbide–encapsulated Be_2C shows substantial promise as a fuel-salt-compatible container material. Be_2C also appears to have high potential to be a long-life, coolant salt–compatible moderator material.

IV.F. Development and Demonstration of the Plant Components and Systems

While progress has been made on key technologies, such as pumps and heat exchangers, for molten salts, component development for commercial-scale systems remains a key challenge that is being addressed by current MSR component and system developers. In general, high-temperature component design has advanced substantially over the past half-century. However, creation of a molten salt component demonstration facility (analogous to the historic liquid-metal engineering center provided in the 1960s to 1970s to support the development of SFRs) to enable vendors to validate commercial-scale component performance is recommended.[49]

IV.G. Remote Inspections, Handling, and Maintenance

Integral designs coupled with a component replacement strategy substantially decrease the remote operations challenges. An integral fuel-salt configuration enables employing an unfueled downcomer region, which would reduce the radiation doses outside of the vessel, as would keeping the fission gases within the vessel for the first couple of days. Technologies for remote operations and maintenance have benefited from decades of sensing and instrumentation development. At the current development status, remote handling and maintenance can be seen more as engineering development issues than research challenges.

The U.S. Nuclear Regulatory Commission's (NRC's) recent decision to develop guidance for near-surface disposal of adequately stabilized, greater-than-Class-C (GTCC) wastes is anticipated to substantially decrease the expense of disposing activated and byproduct materials from MSRs.[50]

A major unresolved issue with inspections is understanding failure precursors. One likely design adaptation to the lack of measurable material failure precursors in MSR components is to reduce the failure consequences through design and operations, i.e., keeping fuel-salt tubes under compression to keep leakage inward. Material surveillance specimens are also likely to play a larger role in first-generation systems.

IV.H. Codes and Standards for High-Temperature Materials

Codes and standards are especially important for materials that perform safety functions. MSRs can substantially reduce the need for high-temperature material codes and standards by avoiding crediting salt-wetted materials to perform safety functions. The NRC has allowed license applicants to choose which containment layers in their design are credited to perform safety functions.[51] A code-qualified, nonnormally salt-wetted guard vessel may provide containment under accident conditions. Existing code-qualified alloys can readily contain fuel salt for the limited durations of accidents.

The prominence of the codes and standards issue in the historic MSBR evaluation is reflective of the safety importance of the pressure-retaining containment layer in LWRs (and to a lesser extent other reactors). The use of code-qualified materials is required for both PWRs and boiling water reactors (*Code of Federal Regulations*, Title 10, Part 50.55a). However, code-qualified materials are not required when the structure does not perform a safety function.

IV.I. Demonstration of Safety Technology

In addition to adequate containment performance, the major safety functions of the proposed system are to provide adequate decay heat rejection and reactivity control. Adequate containment performance at MSRs will be similar to other low-pressure NPPs, mostly dependent on adequate quality in design, construction, operation, and maintenance. Containment and cooling of cover gases will be of greater significance for MSRs due to the much larger quantities of short-lived fission products within the gases.

Natural circulation decay heat removal outside of the salt environment is similar to that of other high-temperature reactors and has been demonstrated in support of high-temperature gas reactor development.[52] A general understanding of buoyancy-driven natural circulation in molten salts is well established, as natural circulation material testing loops have been commonly employed for decades in MSR development. Integral effects testing of overall decay heat removal system performance demonstration, however, may still be necessary to meet the confidence expectation, e.g., *Code of Federal Regulations*, Title 10, Part 50.43(e)(1) for a safety feature at a new reactor.

Large, TS-MSRs have the potential to have a slow-acting, positive moderator temperature-reactivity coefficient.[53] While the positive moderator coefficient can be eliminated through the addition of a neutron poison with an appropriate resonance absorption (e.g., ^{167}Er), all poisons decrease neutronic efficiency. Alternatively, liquid fuel enables passive, temperature-driven defueling of the critical circuit, resulting in a large, rapid net negative temperature-reactivity coefficient. While thermally triggered fluid transfers are well known, any safety system at a NPP will require adequate evaluation and demonstration.

V. PUBLIC-PRIVATE PARTNERSHIP

Private sector actors will be the owners/operators of commercial MSRs, and accordingly, will have leadership of latter stage development and deployment efforts. The public sector, however, retains key roles in enabling private sector success as well as in guiding development toward systems that promote primarily nonfinancial, governmental objectives, such as efficient safety evaluation,

long-term sustainability, and high degrees of safeguards ability and proliferation resistance. MSRs remain less technically mature than other advanced reactors, largely as a result of never receiving the same scale of development resources as other advanced reactor classes. While the historic MSBR program provides a solid technical base, MSR commercialization would benefit substantially from sustained, cross-cutting, foundational technology research and development (R&D).

Thermal-spectrum MSRs require intensive fuel-salt processing to achieve breeding gain. While early-stage fuel stage processing technology would likely be suitable for open development, detailed fuel processing R&D that involves fissile material separation, however, would be restricted so much as to necessitate substantial public sector involvement.

The U.S. government has not invested in MSR fuel processing technologies for nearly half a century. However, the rest of the world has not stood still. The recommended aluminum alloy–based actinide co-separation technology derives from the French fuel processing program. Having a technically and economically attractive, highly proliferation-resistant breeding fuel cycle is strategically important to the United States to provide an alternative to the proliferation-vulnerable fuel cycles being promoted by other nations. Without such an alternative, developing nations are much more likely to choose to pursue fuel cycle technologies with substantially greater proliferation risks. Developing an alternative breeding fuel cycle that does not include producing material more attractive than LEU would enable the United States to maintain strategic leadership as advanced reactor usage expands worldwide.

V.A. MSR Comparative Costs

Advanced reactors are being reconsidered largely because of their potential cost advantages while retaining the near-zero emissions, excellent safety, and dependability of the current fleet. While MSRs offer the potential for substantially lower costs, MSR technology is insufficiently mature for a detailed cost analysis. Hence, the following discussion remains at a high-level, focused on primary cost drivers.

Much of the cost escalation that has occurred with the current fleet is a result of increased safety expectations. The safety analyses of the progressively larger LWRs of the 1950s to 1970s indicated a nontrivial potential for catastrophic accidents and resulted in significant changes in plant design and regulatory oversight.[54] The excellent safety of modern, large, water-cooled reactors has come at the cost of massive, complex, highly engineered safety systems accompanied by a detailed, time-consuming regulatory process. MSRs, in contrast, will rely on a combination of low-pressure, natural convection cooling, and negative reactivity feedback mechanisms (including their unique ability to passively defuel) to achieve their safety performance.[55] MSRs offer the potential of maintaining the excellent safety of modern LWRs while relying on simpler, less massive, less expensive, passive systems.

Potential MSR accidents (for reasonably designed, constructed, operated, and maintained plants) do not result in conditions that cannot be reasonably contained. Thus, MSRs offer the potential of returning to the much simpler maximum credible accident safety adequacy paradigm employed prior to the credible potential for catastrophic accidents becoming apparent at large LWRs.

Construction time is a key cost driver for NPPs. Less massive, simpler components make MSRs well suited to take advantage of the cost and schedule advantages of modular, factory-based construction. MSRs have multiple additional advantageous cost characteristics, such as the lack of need for highly engineered fuel and eventually enrichment services in the case of breeder reactors (about half of the front-end fuel cycle costs at LWRs).[56] Fuel-salt quality assurance may be as simple as measuring its isotopic composition.

The indefinite fuel-salt lifetime and lack of an actinide-bearing waste stream would also decrease back-end fuel cycle costs. It is anticipated that the NRC's recent decision to develop performance-based rules for the near-surface, land disposal of transuranic and GTCC waste (SRM-SECY-20-0098) coupled with the DOE NE's development of grout technology for creating mechanically and chemically stable and robust waste forms could significantly decrease the cost of both the operational and eventual decommissioning of waste streams of MSRs.[57,58]

The need for additional batches of fissile material to initiate the fuel cycle will be an additional upfront cost. However, halide fuel salt has much lower fissile material content than oxide or metal fuels. The dilute nature of the fuel minimizes self-shielding, making all the fissile material immediately useful. The ability to add additional fissile material while online avoids the need for reactivity poisons, and the optimized core design minimizes parasitic resonance absorption as the neutrons thermalize. Fuel salt is a synthesized bulk chemical, not a highly engineered manufactured product, significantly decreasing its cost. Configuring the fuel-salt loop as a natural

circulation loop in vessel minimizes the amount of fuel salt outside of the core. The equilibrium refueling feedstock materials are natural uranium and thorium, so fissile separation costs are only incurred for the initial set of fuel-salt batches.

Other reactor classes do not need to include a coupled chemical processing facility. The chemical processing structures, systems, and components (SSCs) will substantially increase the plant footprint and cost. Moreover, their technologies remain immature, with substantial remaining development risks. The chemical processing SSCs will be highly contaminated. Maintenance and replacement operations will need to be performed remotely, which will increase costs. The large plant unknowns have significant potential to (at least initially) adversely impact plant reliability.

Both beryllium and isotopically separated lithium (^{7}Li) represent significant costs to TS-MSBRs. The price of these materials in industrial quantities remains substantially uncertain as production would have to be significantly scaled up for TS-MSBR deployment. The DOE's Office of Science has recently sponsored the development of substantially improved technology for separating lithium isotopes.[59] While the new technology appears very promising, it has not been developed into an engineering-scale system or commercialized.

Overall, MSBRs have attractive features that may enable cost-effective energy production. However, their technologies and plant configurations remain sufficiently immature to inhibit reasonable uncertainty cost estimation.

VI. CONCLUSIONS AND RECOMMENDATIONS

Thermal-spectrum, liquid-fueled MSRs have long been recognized as having very high potential capabilities (see Fig. 24) for commercial power production with low fissile material resource requirements. Their passive safety and low pressure will decrease construction and regulatory costs. Breeding additional fissile material within a blended Th-U and U-Pu fuel cycle that does not include material more attractive than LEU would enable MSRs to supply a substantial fraction of the world's energy requirements indefinitely.

Molten salt reactors are beginning to attract private capital and are anticipated to be able to attract substantially larger quantities once foundational, high-risk development and demonstration have been performed. Pathways for resolution of all known technical issues have now been identified, and key MSR technologies have advanced substantially in the half-century since the cancellation of the historic MSBR program.

However, significant technological elements remain immature, never having had the necessary sustained development focus to realize their potential. The DOE

Fig. 24. Beecher Briggs transferring mantel of responsibility to Paul Haubenreich upon his retirement (ORNL photo 98031—approved for public release).

NE remains the key actor needed to support and coordinate focused technology development to enable private industry to bring MSBRs to market.

Acknowledgments

This manuscript has been authored by Battelle Energy Alliance, LLC under Contract No. DE-AC07-05ID14517 with the U.S. Department of Energy. The U.S. Government retains and the publisher, by accepting the article for publication, acknowledges that the U.S. Government retains a nonexclusive, paid-up, irrevocable, world-wide license to publish or reproduce the published form of this manuscript, or allow others to do so, for U.S. Government purposes.

Disclosure Statement

No potential conflict of interest was reported by the authors.

Funding

This work was supported by the U.S. Department of Energy Office of Nuclear Energy.

ORCID

David E. Holcomb http://orcid.org/0000-0001-8263-4661
Mauricio E. Tano http://orcid.org/0000-0003-3417-3869

References

1. J. R. ENGEL et al., "Molten-Salt Reactors for Efficient Nuclear Fuel Utilization Without Plutonium Separation," ORNL/TM-6413, Oak Ridge National Laboratory (1978); http://doi.org/10.2172/6650305.
2. J. A. LANE, H. G. MACPHERSON, and F. MASLAN, *Fluid Fuel Reactors*, Addison-Wesley Publishing Co, Boston, Massachusetts (1958); https://egeneration.org/wp-content/Repository/Fluid_Fueled_Reactor_Book/FLUID%20FUEL%20REACTORS.pdf (accessed Nov. 15, 2024).
3. E. P. WIGNER, A. M. WEINBERG, and G. YOUNG, "Preliminary Calculations on a Breeder with Circulating Uranium," ORNL-CF-45-5-347, Oak Ridge National Laboratory (1945).
4. E. S. BETTIS et al., "The Aircraft Reactor Experiment—Design and Construction," *Nucl. Sci. Eng.*, **2**, *6*, 804 (1957); http://doi.org/10.13182/NSE57-A35495.
5. "Report of the Fluid Fuel Reactors Task Force," TID-8507, U. S. Atomic Energy Commission (1959); https://moltensalt.org/references/static/downloads/pdf/TID-8507.pdf (accessed Nov. 15, 2024).
6. J. L. COLLINS et al., "Carbonate Thermochemical Cycle for the Production of Hydrogen," US Patent 7,666,387 B2 (2010); https://www.researchgate.net/publication/236520239_Carbonate_Thermochemical_Cycle_for_the_Production_of_Hydrogen (accessed Nov. 15, 2024).
7. C. FORSBERG, B. E. DALE, and E. INGERSOLL, "Replacing All Fossil Fuels with Nuclear-Enabled Hydrogen, Cellulosic Hydrocarbon Biofuels, and Dispatchable Electricity," *ASME Open J. Eng.*, **3**, 031004 (2024); https://asmedigitalcollection.asme.org/openengineering/article-pdf/doi/10.1115/1.4064592/7254550/aoje_3_031004.pdf (accessed Nov. 15, 2024).
8. H. RITCHIE and P. ROSADO, "Nuclear Energy," OurWorldinData.org (2022); https://ourworldindata.org/nuclear-energy (accessed Nov. 15, 2024).
9. J. CHOE et al., "Fuel Cycle Flexibility of Terrestrial Energy's Integral Molten Salt Reactor (IMSR®)," presented at the 38th Annual Conf. of the Canadian Nuclear Society and 42nd Annual CNS/CAN Student Conf., Saskatoon, Saskatchewan, Canada, June 3–6, 2018; https://inis.iaea.org/search/searchsinglerecord.aspx?recordsFor=SingleRecord&RN=50012947 (accessed Nov. 15, 2024).
10. W. A. BUDD, "Shippingport Operations with the Light Water Breeder Reactor Core. (LWBR Development Program," WAPD-TM-1542, Bettis Atomic Power Laboratory (1986); https://doi.org/10.2172/5914091.
11. "Nuclear Fuel Cycle Evaluation and Screening," Idaho National Laboratory; https://fuelcycleevaluation.inl.gov/SitePages/Home.aspx (accessed 15, 2024).
12. A. M. PERRY and A. W. WEINBERG, "Thermal Breeder Reactors," *Annu. Rev. Nucl. Sci.*, **22**, *1*, 317 (1972); http://doi.org/10.1146/annurev.ns.22.120172.001533.
13. P. VICENTE-VALDEZ JR et al., "Modeling Molten Salt Reactor Fission Product Removal with SCALE," ORNL/TM-2019/1418, Oak Ridge National Laboratory (2020); http://doi.org/10.2172/1608211.
14. P. R. KASTEN, "The MOSEL Reactor Concept," presented at the 3rd Int. Conf. on the Peaceful Uses of Atomic Energy, Geneva, Switzerland, August 31–September 9, 1964.
15. D. G. ESKIN, "Overview of Ultrasonic Degassing Development," *Light Metals* (2017); https://doi.org/10.1007/978-3-319-51541-0_171.
16. O. CONOCAR et al., "Promising Pyrochemical Actinide/Lanthanide Separation Processes Using Aluminum," *Nucl. Sci. Eng.*, **153**, *3*, 253 (2006); http://doi.org/10.13182/NSE06-A2611.
17. L. CASSAYRE et al., "Recovery of Actinides from Actinide-Aluminum Alloys by Chlorination: Part I,"

J. Nucl. Mater., **414**, *1*, 12 (2011); http://doi.org/10.1016/j.jnucmat.2011.04.02.

18. P. SOUČEK et al., "Recovery of Actinides from Actinide-Aluminum Alloys by Chlorination: Part II," *J. Nucl. Mater.*, **447**, *1–3*, 38 (2014); http://doi.org/10.1016/j.jnucmat.2013.12.011.
19. R. MEIER et al., "Recovery of Actinides from Actinide-Aluminum Alloys by Chlorination: Part III - Chlorination with HCl(g)," *J. Nucl. Mater.*, **498**, 213 (2018); http://doi.org/10.1016/j.jnucmat.2017.09.045.
20. Y. K. ZHONG et al., "In-situ Anodic Precipitation Process for Highly Efficient Separation of Aluminum Alloys," *Nat. Commun.*, **12**, *1*, 5777 (2021); http://doi.org/10.1038/s41467-021-26119-9.
21. B. D. KAGAN et al., "Synthesis of Actinide Fluoride Complexes Using Trimethyltin Fluoride as a Mild and Selective Fluorinating Reagent," *Eur. J. Inorg. Chem.*, **2018**, *11*, 1247 (2018); http://doi.org/10.1002/ejic.201701232.
22. S. CHONE and B. J. RILEY, "Thermal Conversion in Air of Rare-Earth Fluorides to Rare-Earth Oxyfluorides and Rare-Earth Oxides," *J. Nucl. Mater.*, **561**, 153538 (2022); http://doi.org/10.1016/j.jnucmat.2022.153538.
23. H. C. SAVAGE and J. R. HIGHTOWER JR, "Engineering Tests of the Metal Transfer Process for Extraction of Rare-Earth Fission Products from a Molten-Salt Breeder Reactor Fuel Salt," ORNL-5176, Oak Ridge National Laboratory (1977); http://doi.org/10.2172/7316028.
24. C. D. SCOTT and W. L. CARTER, "Preliminary Design Study of a Continuous Fluorination–Vacuum-Distillation System for Regenerating Fuel and Fertile Streams in a Molten Salt Breeder Reactor," ORNL-3791, Oak Ridge National Laboratory (1966); http://doi.org/10.2172/4527528.
25. A. T. PEACOCK, W. J. HAWS, and M. A. PICK, "Development of Beryllium-Carbide Fibre Reinforced Beryllium for Fusion Applications," *Proc. 15th IEEE/NPSS Symp. on Fusion Engineering-Supplement*, p. 50, Institute of Electrical and Electronics Engineers (1993).
26. B. F. WEAVER et al., "Phase Equilibria in Molten Salt Breeder Reactor Fuels—I. The System LiF- BeF2-UF4-ThF4," ORNL-2896, Oak Ridge National Laboratory (1961); http://doi.org/10.2172/4081840.
27. *IAEA Safeguards Glossary*, 2022 ed. International Nuclear Verification Series No. 3 (Rev. 1), Table 2—Estimated Material Conversion Times for Finished Pu or U Metal Components, International Atomic Energy Agency (2022); https://www-pub.iaea.org/MTCD/publications/PDF/PUB2003_web.pdf (accessed Nov. 15, 2024).
28. O. CONOCAR et al., "Promising Pyrochemical Actinide/Lanthanide Separation Processes Using Aluminum," *Nucl. Sci. Eng.*, **153**, *3*, 253 (2006); http://doi.org/10.13182/NSE06-A2611.
29. O. CONOCAR, N. DOUYERE, and J. LACQUERMENT, "Extraction Behavior of Actinides and Lanthanides in a Molten Fluoride/Liquid Aluminum System," *J. Nucl. Mater.*, **344**, *1–3*, 136 (2005); http://doi.org/10.1016/j.jnucmat.2005.04.031.
30. F. R. CLAYTON, G. MAMANTOV, and D. L. MANNING, "Electrochemical Studies of Uranium and Thorium in Molten LiF-NaF-KF at 500°C," *J. Electrochem. Soc.*, **121**, *1*, 86 (1974); https://iopscience.iop.org/article/10.1149/1.2396838 (accessed Nov. 15, 2024).
31. J. L. KLOOSTERMAN, "HTR Design Aspects," Jan Leen Kloosterman; http://www.janleenkloosterman.nl/gen4fin_201009.php (accessed Nov. 15, 2024).
32. E. S. BETTIS et al., "Design: Chapter 5 of Molten-Salt Reactor Program Semi Annual Progress Report for Period Ending February 29, 1968," ORNL-4254, Oak Ridge National Laboratory (1968); https://moltensalt.org/references/static/downloads/pdf/ORNL-4254.pdf (accessed Nov. 15, 2024).
33. E. S. BETTIS et al., "Design, Chapter 5 of Molten-Salt Reactor Program Semi Annual Progress Report for Period Ending August 31, 1967," ORNL-4191, Oak Ridge National Laboratory (1967); https://moltensalt.org/references/static/downloads/pdf/ORNL-4191.pdf (accessed Nov. 15, 2024).
34. H. MORIYAMA, S. TANAKA, and K. NODA, "Irradiation Effects in Ceramic Breeder Materials," *J. Nucl. Mater.*, **258–263**, *1*, 587 (1998); http://doi.org/10.1016/S0022-3115(98)00108-1.
35. K. NODA et al., "Irradiation Effects on Lithium Oxide," *J. Nucl. Mater.*, **123**, *1–3*, 908 (1984); http://doi.org/10.1016/0022-3115(84)90193-4.
36. I. MAYA et al., "Inertial Confinement Fusion Reaction Chamber and Power Conversion System Study. Final Report," UCRL-15750, GA-A-17842, General Atomics Technologies, Inc (1985); http://doi.org/10.2172/6021627.
37. R. H. MARION and W. A. MUENZER. "Development of Be_2C-Graphite-UC_2 Fuel for Pulsed Reactors," presented at the ANS annual meeting, San Diego, California, June 18, 1978.
38. M. H. FELDMAN and L. SILVERMAN, "Chemical Stability of Be_2C under Cyclotron Irradiation," NAA-SR-114, Atomic Energy Research Development (1951); http://doi.org/10.2172/4338451.
39. A. A. CAMPBELL et al., "Be_2C Synthesis, Properties, and Ion-Beam Irradiation Damage Characterization," ORNL/TM-2023/3011, Oak Ridge National Laboratory (2023); http://doi.org/10.2172/1997705.
40. J. F. QUIRK, "Chapter 1.5 Beryllium Carbide," *The Reactor Handbook*, Vol. 3, Section 1, General Properties, J. F. HOGERTON and R. C. GRASS, Eds. pp. 101–103, AECD-3647, Atomic Energy Commission (1953); http://doi.org/10.2172/4384109.

41. A. M. SAUL and W. J. SMITH, "Available Information on Be_2C," NAA-SR-MEMO-1702, Atomic Energy Research Development (1956); http://doi.org/10.2172/1364768.

42. K. BARRETT, S. BRAGG-SITTON, and D. GALICKI, "Advanced LWR Nuclear Fuel Cladding System Development Trade-Off Study," INL/EXT-12-27090, Idaho National Laboratory (2012); https://inldigitallibrary.inl.gov/sites/sti/sti/5554576.pdf (accessed Nov. 15, 2024).

43. I. L. SHABALIN, *Ultra-High Temperature Materials II: Refractory Carbides I (Ta, Hf, Nb and Zr Carbides)*, Springer, Berlin (2019); https://link.springer.com/book/10.1007/978-94-024-1302-1 (accessed Nov. 15, 2024).

44. C. ANG, L. SNEAD, and K. BENENSKY, "Niobium Carbide as a Technology Demonstrator of Ultra-High Temperature Ceramics for Fully Ceramic Microencapsulated Fuels," *Int. J. Ceram. Eng. Sci.*, **1**, *2*, 92 (2019); http://doi.org/10.1002/ces2.10014.

45. "An Evaluation of the Molten Salt Breeder Reactor," WASH-1222, U.S. Atomic Energy Commission Division of Reactor Development and Technology (1972); http://doi.org/10.2172/4372873.

46. R. C. ROBERTSON, "Conceptual Design Study of a Single-Fluid Molten-Salt Breeder Reactor," ORNL-4541, Oak Ridge National Laboratory (1971); http://doi.org/10.2172/4030941.

47. J. R. KEISER, "Status of Tellurium-Hastelloy N Studies in Molten Fluoride Salts," ORNL/TM-6002, Oak Ridge National Laboratory (1977); http://doi.org/10.2172/7295251.

48. "Molten Salt Thermal Properties Databases," Oak Ridge National Laboratory; https://sc.edu/study/colleges_schools/engineering_and_computing/docs/research/mstdb_access.pdf (accessed Nov. 15, 2024).

49. "Energy Technology Engineering Center," EM Consolidated Business Center, U.S. Department of Energy; https://www.etec.energy.gov/Operations/Operations_History.php (accessed Nov. 15, 2024).

50. "Greater-Than-Class C and Transuranic Waste," U. S. Nuclear Regulatory Commission (last modified April 26, 2023); https://www.nrc.gov/waste/llw-disposal/llw-pa/gtcc-transuranic-waste-disposal.html (accessed Nov. 15, 2024).

51. A. L. VIETTI-COOK, "Staff Requirements—SECY-18-0096—Functional Containment Performance Criteria for Non-Light-Water-Reactors," Official Memorandum, US Nuclear Regulatory Commission (2018); https://www.nrc.gov/docs/ML1833/ML18338A502.pdf (accessed Nov. 15, 2024).

52. D. LISOWSKI et al., "Technical Letter Report: An Overview of Non-LWR Vessel Cooling Systems for Passive Decay Heat Removal (Final Report)," ANL/NSE-21/3, Argonne National Laboratory (2021); https://www.nrc.gov/docs/ML2113/ML21139A048.pdf (accessed Nov. 15, 2024).

53. D. LECARPENTIER et al., "Temperature Feedbacks of a Thermal Molten Salt Reactor: Compromise Between Stability and Breeding Performances," *Proc. ICAPP*, Vol. 3, p. 4, Córdoba, Spain, May 4–7, 2003 (2003); https://www.researchgate.net/publication/281072196_Temperature_feedbacks_of_a_thermal_molten_salt_reactor_Compromise_between_stability_and_breeding_performances (accessed Nov. 15, 2024).

54. B. L. COHEN, "Chapter 9: Costs of Nuclear Power Plants —What Went Wrong?," *The Nuclear Energy Option*, Plenum Press (1990); http://www.phyast.pitt.edu/~blc/book/ (accessed Nov. 15, 2024).

55. D. E. HOLCOMB et al., "Molten Salt Reactor Fundamental Safety Function PIRT," ORNL/TM-2021/2176, Oak Ridge National Laboratory (2021); https://info.ornl.gov/sites/publications/Files/Pub165504.pdf (accessed Nov. 15, 2024).

56. "Economics of Nuclear Power," World Nuclear Association (2023); https://world-nuclear.org/information-library/economic-aspects/economics-of-nuclear-power.aspx (accessed Nov. 15, 2024).

57. B. P. CLARK, "Path Forward and Recommendations for Certain Low-Level Radioactive Waste Disposal Rulemakings," Official Memorandum SRM-SECY-20-0098, U.S. Nuclear Regulatory Commission (2022); https://www.nrc.gov/docs/ML2209/ML22095A227.pdf (accessed Nov. 15, 2024).

58. J. R. HARBOUR, "Summary of Grout Development and Testing for Single Shell Tank Closure at Hanford," WSRC-TR-2005-00195, Savannah River National Laboratory (2005); http://doi.org/10.2172/881527.

59. Z. ZHANG et al., "High-efficiency Lithium Isotope Separation by Electrochemical Deposition and Intercalation with Electrochemical Isotope Effect in Propylene Carbonate and [BMIM][DCA] Ionic Liquid," *Electrochim. Acta*, **361**, 137060 (2020); http://doi.org/10.1016/j.electacta.2020.137060.